

DOE/OR/21400--7491

C/ORNL 92 0083

ornl

**OAK RIDGE
NATIONAL
LABORATORY**

MARTIN MARIETTA

**CRADA Final Report
for
CRADA Number ORNL92-0083**

**A NEW METHOD FOR MEASURING THE
DYNAMICSURFACE TENSION OF COMPLEX-MIXTURE
LIQUID DROPS**

**Xiaoguang Zhang, M. T. Harris, and O. A. Basaran
Oak Ridge National Laboratory**

Spray Drift Task Force

**Approved for public release;
distribution is unlimited.**

**MANAGED BY
MARTIN MARIETTA ENERGY SYSTEMS, INC.
FOR THE UNITED STATES
DEPARTMENT OF ENERGY**

DISTRIBUTION OF THIS DOCUMENT IS UNLIMITED *JR*

CONFIDENTIAL

DISCLAIMER

**Portions of this document may be illegible
in electronic image products. Images are
produced from the best available original
document.**

C/001 ORNL--92-0083

MARTIN MARIETTA

MARTIN MARIETTA ENERGY SYSTEMS, INC.

POST OFFICE BOX 2009
OAK RIDGE, TENNESSEE 37831

November 28, 1994

Mr. Peter D. Dayton
Director, Procurement and Contracts
Department of Energy, Oak Ridge Operations
Post Office Box 2001
Oak Ridge, Tennessee 37831-2001

Dear Mr. Dayton:

Final Report for CRADA No. ORNL92-0083 with Spray Drift Task Force

The subject CRADA has been completed and enclosed is the Final Report for this project.

This report does not contain proprietary information or Protected CRADA Information. Neither Energy Systems nor the participant object to public distribution of this report.

If you have any questions, please feel free to contact me.

Very truly yours,

C. A. Vebert

jk
Brian Bovee
Business Manager
Office of Technology Transfer

BBB:cav

Enclosure - As Stated.

cc: File - RC

DISCLAIMER

This report was prepared as an account of work sponsored by an agency of the United States Government. Neither the United States Government nor any agency thereof, nor any of their employees, makes any warranty, express or implied, or assumes any legal liability or responsibility for the accuracy, completeness, or usefulness of any information, apparatus, product, or process disclosed, or represents that its use would not infringe privately owned rights. Reference herein to any specific commercial product, process, or service by trade name, trademark, manufacturer, or otherwise does not necessarily constitute or imply its endorsement, recommendation, or favoring by the United States Government or any agency thereof. The views and opinions of authors expressed herein do not necessarily state or reflect those of the United States Government or any agency thereof.

Report to be submitted to
SPRAY DRIFT TASK FORCE
as part of a CRADA between ORNL/MMES and SDTF entitled:
**A NEW METHOD FOR MEASURING THE DYNAMIC SURFACE
TENSION OF COMPLEX-MIXTURE LIQUID DROPS†**

Final report due at the end of Phase 4:
**STANDARD OPERATING PROCEDURES AND SUMMARY
OF KEY MEASUREMENTS AND FINDINGS OF THE CRADA**

**Xiaoguang Zhang, Michael T. Harris, and
Osman A. Basaran**

**Chemical Technology Division
Oak Ridge National Laboratory
Oak Ridge, Tennessee 37831**

June 29, 1994

EXECUTIVE SUMMARY

This report describes a new experimental technique that has been developed to measure the dynamic surface tension at the interface of a drop of a range finding fluid growing or forming into air from the end of a fine capillary and summarizes key measurements and findings made with the new technique. The report has been written in such a way that it assumes no prior familiarity with the new technique or previous reports issued under this CRADA.

Although this report concludes the formal portion of the work performed under this CRADA, the ORNL researchers shall continue to collaborate with and assist members of the SDTF on an informal basis. Future activities carried out in this manner might include performing limited sets of measurements for the SDTF with the new technique for comparison with other available techniques and making our laboratories available to SDTF researchers for short term training on the ORNL equipment.

†CRADA work sponsored by and in collaboration with the Spray Drift Task Force and the Divisions of Chemical Sciences (O. A. Basaran), Advanced Energy Projects (M. T. Harris), and Material Sciences (M. T. Harris), Office of Basic Energy Sciences, U.S. Department of Energy under contract DE-AC05-84OR21400 with Martin Marietta Energy Systems, Inc.

ABSTRACT

A simple and accurate technique has been developed for measuring dynamic surface tension. The new technique is based on growing a drop at the end of a fine capillary into another immiscible fluid and can follow the changes in tension at a freshly formed interface during its entire period of evolution. When the relative importance of the surface tension force is large compared to gravitational and viscous forces, shapes of growing drops are sections of spheres and the difference in pressure between the interior and the exterior of the drop Δp is related to the surface tension σ and the radius of curvature R by the static Young-Laplace formula $\Delta p = 2\sigma/R$. In contrast to related work (17-19), the new technique can determine the surface tension of an interface with a surface age of a few to tens of milliseconds by measuring transient drop shapes and pressures in 1/6 to 1 millisecond. The capabilities of the new method are demonstrated by performing tension measurements on liquid systems that do not exhibit dynamic surface tension as well as ones that exhibit significant dynamic tension effects. Tension measurements made with surfactant-laden solutions show that variation of surface tension is nonmonotonic in time. In such systems, the dynamic behavior of surface tension is shown to depend upon both the rate of interfacial dilatation and that of surfactant transport. A maximum in the surface tension is attained when the lowering of the surfactant concentration on the drop interface due to its dilatation is balanced by the addition of fresh surfactant to the interface by convection and diffusion. During the early stages of drop growth, the newly forming drop undergoes oscillations the amplitude and frequency of which decrease with time. Consequently, the reported simple to apply but powerful technique for the measurement of surface tension that relies on the use of the Young-Laplace formula can be used only after the oscillations are damped out completely, unless a comprehensive modification is applied.

1. INTRODUCTION

In many separation and extraction processes *and* spraying and ink-jet printing applications, a fluid is ejected from a nozzle or an orifice into another immiscible fluid. At low flowrates, the fluid being ejected emanates from the nozzle as discrete droplets (1). At high flowrates, the fluid is ejected from the nozzle as a jet which subsequently breaks up into small drops due to the well known Rayleigh instability (1). Surface tension, as one of key "solution" properties, competes with other relevant forces that may be operating, e.g., inertial, viscous, viscoelastic or electric, to control the dynamics of the drop formation or jetting process and set the final drop size distribution.

The tension at a freshly formed interface, as the surface of a forming drop or a breaking jet, may be quite different from the equilibrium or static value and may vary as a function of time, if surface active materials are present. The dynamic property of the surface tension (often referred to as dynamic surface tension) is dependent on the instant composition of surface active materials accumulated on the interface. The value of the surface tension usually decreases monotonically with an increase in the concentration of surfactant absorbed on the interface until an equilibrium concentration is eventually reached at which point the surface tension tends to its equilibrium value. Most industrially relevant drop formation and atomization processes occur in a time frame on the order of a few milliseconds or less, over which equilibrium conditions are not attained and dynamic tension plays a major role. This short time scale over which a measurement has to be made and the large amounts of surface area that are created in these practical situations render inapplicable most existing techniques of measuring dynamic surface tension. Thus, the major goal of this work is to present a new technique for measuring dynamic surface tension over an effective surface age of a few milliseconds and longer under conditions that closely approximate practical

conditions.

Efforts for measuring dynamic surface tension have been around for a century. A recent and comprehensive summary can be found in the book by Edwards *et al.* (2). Some of the currently used techniques are based on observations of interfacial waves at a fluid/fluid interface to measure surface dilatational elasticity and surface tension. These include the longitudinal wave technique (3, 4), laser light-scattering (5), Langmuir trough (6), and the oscillating bubble (7). As the interface is typically only slightly perturbed from its equilibrium state, these techniques are of little value in measuring the dynamic surface tension at the interface of a growing drop. A technique based on the phenomenon of Rayleigh instability is the oscillating jet method (8, 9) due to the famous physicist Niels Bohr (10). With the many assumptions that are made in deriving the working equation of this method, the large scatter in the resultant surface tension data limits its usefulness. In addition, as the interface wave methods, this technique works best for low viscosity or virtually inviscid fluids. The viscosities of many practically important fluids can be large enough that the oscillations can get damped out within a few milliseconds (11), thereby rendering measurements based on the oscillating jet method totally impossible. The so-called maximum bubble pressure method (12-14) and dynamic drop volume methods (15, 16) are other widely used techniques for measuring dynamic surface tension because of their apparent simplicities. One drawback of these methods is that they only furnish the value of the dynamic surface tension at one certain instant in time and not during the entire process of drop/bubble formation. Therefore, these methods are not suitable to explore the actual transient evolution of tension on a single drop interface.

Therefore, a more general technique for measuring dynamic surface tension was developed and is described in this work that is based on growing a drop at the end of a fine capillary into another immiscible fluid, as shown in figure 1. The technique relies

on measuring simultaneously the instantaneous pressure inside and the radius of curvature of the drop as it grows. First, the technique is capable of making measurements in as little as a few milliseconds or in as long as hours. Second, it is capable of monitoring the change in tension at the freshly formed interface of a drop during its entire period of evolution. In this work, we go beyond existing similar techniques proposed by others (17-19) by focusing on the early times of drop formation, in particular on the period preceding the hemispherical stage. To make such measurements, advantage is taken of an ultra high-speed video camera and a data link system. Moreover, use of the video camera in conjunction with a digital image analysis system allows measurement of the real shape, or size, of a drop as a function of time during drop growth. This capability makes the determination of the drop size completely independent of how the pressure varies inside the drop and the manner in which the drop fluid wets the capillary, which are other advantages of the present technique over the works of others (17, 19). Yet another goal of the present work is to determine the limitations of the growing drop technique, which have heretofore remained inadequately explored. In particular, this work examines such issues as the earliest time (measured from zero surface age) after which the technique can furnish accurate surface tension data and the effect of drop viscosity on surface tension measurements.

Section 2 presents scaling arguments that set limits on physical properties and capillary radii for ensuring that forming drops grow as sections of spheres. Section 3 describes the experimental apparatus, materials and the methods of data acquisition and analysis. Section 4 shows that the new technique is extremely well suited for inferring dynamic surface tension. First the accuracy of the new method is demonstrated by measuring the surface tension of well characterized liquid systems — the interface between a growing drop of pure water, water plus propanol, and water plus glycerol and air — that do not exhibit dynamic tension effects. Next the capability

of the new method to measure dynamic surface tension is displayed by measuring the tension at the interface of a drop of water plus a surfactant forming into air. Moreover, oscillations of the interface between air and newly-formed drops of liquids of different viscosities are discussed in light of the measured drop shape and pressure data. Concluding remarks are the subject of section 5.

2. PHYSICS OF GROWING DROPS: SCALING ARGUMENTS AND GOVERNING EQUATIONS

Motion of a Newtonian fluid of viscosity μ and density ρ inside a growing drop is governed by the Navier-Stokes system, which is nondimensionalized by using the radius of the capillary a as length scale and the maximum fluid velocity inside the capillary u as velocity scale:

$$\tilde{\nabla} \cdot \tilde{\mathbf{v}} = 0, \quad [1]$$

$$Re \left(\frac{\partial \tilde{\mathbf{v}}}{\partial \tilde{t}} + \tilde{\mathbf{v}} \cdot \tilde{\nabla} \tilde{\mathbf{v}} \right) = \tilde{\nabla} \cdot \underline{\underline{\tilde{T}}} + \frac{G}{Ca} \mathbf{e}_z, \quad [2]$$

where $\tilde{\mathbf{v}}$ is the dimensionless velocity, $\underline{\underline{\tilde{T}}}$ is the dimensionless stress tensor, \tilde{t} is the dimensionless time, and \mathbf{e}_z denotes the unit vector along the direction of gravity, which is taken to be the z -direction. In equation [2], $Re \equiv \frac{\rho u a}{\mu}$ is the Reynolds number, $G \equiv \frac{\rho a^2 g}{\sigma^*}$ is the gravitational Bond number, and $Ca \equiv \frac{\mu u}{\sigma^*}$ is the capillary number, where g is the acceleration due to gravity and σ^* is a characteristic surface tension, e.g. that of the pure solvent. Re measures the importance of inertial forces relative to viscous forces, G measures the importance of gravitational forces relative to surface tension forces, and Ca measures the importance of viscous forces relative to surface tension forces. It is well known that the profile of a static drop pendant from a capillary is a section of a sphere provided that $G \ll 1$ (20). By contrast, the profile of a growing drop is also shaped by the competition between viscous and surface

tension forces. Our recent theoretical studies (21) have shown that $Ca \ll 1$ also to ensure that the profile of a growing drop is a section of a sphere. Under the condition of small gravitational Bond and capillary numbers, surface tension forces dominate gravitational and viscous forces and enforce a growing drop to maintain its spherical shape. With a capillary of small enough radius and, thus, a drop of small enough radius, the restrictions of small gravitational Bond and capillary numbers are well satisfied when $G < 0.03$ and $Ca < 0.004$ in our experiments, as discussed in sections 3 and 4 of this report. Therefore, the assumption that the shape of a growing drop is spherical can be safely applied throughout the present work, a fact that is further reinforced by taking pictures of growing drops in the experiments. As shown below, the existence of a spherical drop greatly facilitates the analysis of dynamic surface tension data. Nevertheless, capillaries of large radii, which lead to growing drops that are nonspherical in shape, can also be used; however, their use would complicate, but not make impossible, the analysis of experimental results, as we show elsewhere (21, 22).

When the drop grows as a section of a sphere, the surface tension, σ , which is assumed to be uniform along the interface of a small drop, can be inferred from the requisite balance of normal stresses on the interface of the spherical drop (cf. (11, 19)), written here in dimensional form:

$$\underline{n} \cdot \underline{n} : (\underline{\mathbf{T}}_{out} - \underline{\mathbf{T}}_{in}) = \frac{2\sigma}{R}, \quad [3]$$

where \underline{n} is an outward pointing unit normal to the interface (i.e., it points from the inside, *in*, to the outside, *out*) and R is the radius of curvature of the drop. At a stretching spherical interface, $\underline{n} \cdot \underline{n} : \underline{\mathbf{T}} = -p + 2\mu \frac{\partial v_R}{\partial R}$, where p is the pressure and v_R is the component of the velocity normal to the interface. Therefore, the stress balance

[3] is reduced to:

$$\Delta p \equiv p_{in} - p_{out} = \frac{2\sigma}{R} + 2\Delta\mu \frac{\partial v_R}{\partial R}, \quad [4]$$

where $\Delta\mu$ is the viscosity difference between the drop and the ambient fluid. The second term on the right side of [4] represents the effect of bulk viscosity on the stress balance. For a purely radial flow, a condition which is commonly assumed to hold when $G \ll 1$ (19), $\frac{\partial v_R}{\partial R} = -\frac{2}{R}v_R = -\frac{2}{R}\frac{dR}{dt}$, where t is the time to form a drop having a radius of curvature R . The time rate of change of R , normalized by R , can be shown to be given by

$$\frac{dR}{Rdt} = \pm \frac{Q}{a^3} \frac{\sqrt{\tilde{R}^2 - 1}}{\pi \tilde{R}^2 (\tilde{R} \pm \sqrt{\tilde{R}^2 - 1})^2}, \quad [5]$$

where $\tilde{R} \equiv R/a$ is the dimensionless radius of curvature of the growing drop scaled by the radius of the capillary and Q is the volumetric flow rate. The negative signs in [5] are used during the pre-hemisphere period and indicate a decrease in the radius of curvature with time until R reaches its minimum when the drop is a hemisphere. The positive signs in [5] are used during the post-hemisphere period. Figure 2 shows the variation of the normalized expansion rate, $\frac{dR}{Rdt}$, as a function of a dimensionless time $\tilde{\tau}$, which is obtained by scaling the actual time by the time that it takes for the drop to reach the hemispherical stage. The normalized expansion rate is seen to increase rapidly from negative infinity during the pre-hemisphere period, to attain a maximum near the time at which the drop is a hemisphere, and then to asymptotically tend toward zero during the post-hemisphere period. The large magnitude of the initial expansion rate can result in significant viscous stresses. However, in the present experiments, measurements of surface tension start from the time at which the drop is nearly hemispherical in shape, i.e. $\tilde{\tau} \simeq 0.6$ in figure 2, as discussed in detail later. Thus, the magnitude of the normalized expansion rate in the experiments is always smaller than 12. By way of example, for a millimeter-sized water drop growing into

air, the surface tension induced stresses are about three to four orders of magnitude as large as viscous stresses. Therefore, viscous stresses can be completely neglected compared to capillary forces and the pressure excess over ambient in the forming drop right inside the moving interface is strictly determined by the curvature of the interface for most low viscosity, Newtonian fluids. For high viscosity fluids, the experimental results of section 4 and the theoretical results of (21, 22) show that viscous stress can play a significant role in determining surface tension even though estimating viscous stress on the assumption of radial flow, $\frac{4\Delta\mu}{R} \frac{dR}{dt}$, would lead to the conclusion that it is negligible compared to capillary pressure. This too is a point to which we return in what follows. Therefore, when stresses due to bulk viscosity and also surface viscosity (see, e.g., (19)) are negligible, [4] simplifies to the static Young-Laplace formula:

$$\Delta p = \frac{2\sigma}{R}. \quad [6]$$

With negligible viscous and gravitational forces, the pressure inside a growing drop, although a function of time, is virtually uniform in space. Hence, the dynamic surface tension can be readily inferred from equation [6] by simply measuring the radius of curvature and the pressure inside the growing drop as a function of time.

3. EXPERIMENTAL APPROACH

In the experiments, a liquid drop is grown from the tip of a capillary at constant volumetric flow rate. This section describes the apparatus used to carry out the measurements and the liquids used in the experiments.

3.1. Apparatus

Figure 3 shows a schematic sketch of the experimental setup. The experimental

apparatus consists essentially of a fine capillary tube from the tip of which a drop is formed or grown, a liquid pump to supply the drop liquid, a pressure transducer to gauge the pressure inside the drop, a video camera for capturing images of the growing drop, and associated hardware for recording, storing and analyzing drop shape and pressure data. The capillary tube is immersed in a glass cell filled with the ambient fluid and the whole apparatus, except for the liquid pump, is placed on a vibration isolation table.

One of the essential pieces of equipment for carrying out the drop formation experiments is an ISCO, Inc. digital syringe pump, model 100DM, that delivers virtually pulseless flow to a fine capillary tube with outstanding stability and precision. The pump can deliver flow rates in the range $0.01 \mu\text{L}/\text{min}$ to $25 \text{ mL}/\text{min}$ with $\pm 0.3\%$ accuracy. Moreover, to ensure that there are no pulsations in flow rate, an Upchurch Scientific model U-445 backpressure regulator is placed downstream of the syringe pump.

In the experiments carried out to date, two types of capillary tubes have been used. The first is a stainless steel nozzle with an outer radius of 0.0397 cm and the other a teflon nozzle with an outer radius of 0.0381 cm . The choice of material for the capillary is important because if the capillary is preferentially wetted by the drop liquid instead of the ambient fluid, the location of the three-phase contact line where the drop, ambient fluid, and the capillary meet is uncertain (19). In particular, the contact line may be (i) pinned on the inner sharp edge of the capillary wall, (ii) pinned on the outer sharp edge of the capillary wall, or (iii) may not be pinned at all, but wet the outer wall of the capillary. The first two situations do not present a problem. The third one, however, renders determination of the radius of curvature of the drop difficult due to the inconsistent changes in the radius of curvature as the contact line moves, and, therefore, was avoided in previous works on growing drops (17, 19). In

the present experiments, the radius of curvature is determined by measuring the real shape of the drop as described below. Therefore, whether the contact line pins on the edge of the capillary is no longer a restriction for making tension measurements. Nevertheless, in order to simplify the analyses of radius and pressure data recorded in the experiments, the materials that the capillary is made of were carefully selected based upon the properties of the fluids used. With water and other aqueous solutions, a stainless steel capillary is used in the experiments which ensures that the drop is pinned to the outer edge of the capillary. Drops of organic liquids wet the outer walls of steel capillaries. For such drops, teflon tubes have been found to ensure that the contact line remains pinned to the sharp outer edge of the capillary.

Another essential piece of equipment is a pressure transducer. The transducer used is model 8510B-1 made by Endevco Corp. which has a measuring range 0 to 1 psig, a response rate of 55 kHz, a sensitivity of 300 mv/psi, and an accuracy of 0.1%. The output signals from the transducer are amplified by a conditioning unit, Endevco Corp. model 160. A converter, Kodak Multi-Channel Data Link, digitizes the signals and transmits them to the motion analysis system described below. The measured electrical signals are converted into pressure units by a linear calibration formula which is determined by means of a hydrostatic pressure calibration. There are of course contributions to the pressure drop measured by the transducer in addition to the Δp in [6]. These occur in the liquid supply line between the transducer and the drop. Extreme care is exercised to measure these before any experimental run is carried out and to subtract the extra pressure drop in determining the tension. Nevertheless, this calibration procedure is straightforward. It is tantamount to running the pump at the flow rate of the drop formation experiment, but without forming drops. The extra pressure drop in the liquid supply lines between the transducer and the tip of the capillary is then determined by just immersing the tip of the capillary into a large

bath that is filled with the same liquid as that of the drop. With these precautions, the instantaneous pressure inside the drops can be measured within an accuracy of ± 0.015 cm H_2O .

The most important and impressive piece of equipment, which sets our experiments apart from those of others, is a high-speed motion analysis/video system for capturing shapes of forming drops. For making tension measurements over very short periods of time, ranging from as few as a fraction of a millisecond to as long as seconds (or longer), a Kodak Ektapro Model EM 1012 Electronic Memory Motion Analyzer and associated video hardware are employed. The Ektapro system is composed of an intensified imager, i.e. the camera, and a processor which can record 1,000 full images or 12,000 partial images per second. Moreover, the Ektapro can display and store side by side the instantaneous drop shape and pressure data. Images of growing drops, along with instantaneous pressures, are later recorded and replayed on a Panasonic model PV-54990 S-VHS recorder. The drop shape and pressure data are viewed on a Sony color video monitor, model PVM-1341. The images are digitized by means of a frame grabber, a Data Translation DT2851 board, that is installed in an IBM-compatible PC, and an edge detection routine is employed to locate the interfacial profile from the digitized image. The image digitization system allows rapid and accurate determination of the loci of interfaces from which the radii of curvature of the growing drops are readily calculated.

In a typical run, the pump and the liquid lines, upon being thoroughly cleaned, are carefully filled with the drop liquid to avoid any air bubbles in the system, which is necessary for eliminating any uncertainty in the liquid flow rate (23). The flow rate is then set to the amount for which the system is calibrated, and the system is allowed to run for about two hours before measurements are taken. A periodic flow situation is then reached in which drops form, grow, and detach from the outlet of the capillary

tube. The experimental time taken for the whole process is sufficiently small, usually about 1 sec but always less than 10 sec, that the changes in the drop size and interface properties due to evaporation of the drop liquid may be safely neglected (24).

3.2. Materials

The drop liquids used in the experiments are either well recognized standards, e.g. triple distilled water by Millipore Corp., 15% (by weight) n-propanol and 85% (by weight) glycerol from EM Science in distilled water, or aqueous surfactant solutions. The surfactants, Triton X-100 and Sodium Dodecyl Sulfate obtained from J. T. Baker Inc., Sodium Dioctyl Sulfosuccinate from Cyanamid, and Induce AL-2700 from ICI Americas Inc., are used without further modification and dissolved in distilled water at the specified concentrations. In all experiments carried out to date, liquid drops form and grow in air and tensions of liquid/air interfaces are measured. The measurements are taken within 8 hours of preparation of the surfactant solutions. All experiments are performed at the room temperature of $22^\circ \pm 0.5^\circ C$.

4. EXPERIMENTAL RESULTS

The typical process of drop formation and growth is illustrated in figure 4 for a drop of distilled water growing out of a steel capillary into air with a flow rate $Q = 100\mu L/min$. Figure 4(a) shows a drop as it is just starting to fall off the capillary. The liquid in the capillary and the drop are reluctant to separate and connected by a throat. A millisecond later, in figure 4(b), the throat is rupturing and the drop is about to detach, which defines the time of zero surface age. As the drop falls, the part of the throat that is left attached to the liquid in the capillary rebounds toward the tube to form a new drop and the pendant drop so formed oscillates as shown in

figure 4(c). As a new drop starts to grow, the oscillations are damped over a period of time. As shown in figure 4(d), no oscillations can be detected on the interface 28 milliseconds after the start of the drop formation process. Figure 4(e) shows that the new forming drop is nearly hemispherical 40 milliseconds later. A larger drop, but one whose profile is still a section of a sphere, is shown 400 milliseconds later in figure 4(f).

4.1. Surface Tension Measurements

Thus, in the surface tension data presented below, for each growing drop time is measured from the time of detachment of the previous drop. However, tension results are not reported in a drop's life until oscillations of the newly-formed drop are completely damped out, evidenced by observing the interface shape and the pressure inside the drop (cf. figure 4(d) and see below). This ensures that there are no oscillation induced uncertainties in the drop radius and pressure. The evolution of surface tension is determined by analyzing drop radius and pressure data from at least 15 different sets of measurements that are selected out of all those made with increasing time during the drop growth process.

Figure 5 shows the instantaneous surface tension at the interface between a growing drop of triple distilled water and air, a growing drop of a mixture of water-15% (by weight) n-propanol and air, and a growing drop of a mixture of water-85% (by weight) glycerol and air. These liquid systems should not exhibit dynamic tension effects and their equilibrium surface tensions are well documented in the literature. For different flow rates, with times ranging between 20 milliseconds and 3,000 milliseconds, figure 5 shows that the measured tension of the water/air interface and that of the water-propanol/air interface do not exhibit dynamic effects. Moreover, the measured values are in excellent agreement with the literature values of 73.0 dyne/cm and 28.3

dyne/cm, respectively (25), which are shown as solid lines in figure 5. As a test, these results demonstrate the capability of the growing drop technique for accurately and reliably measuring the instantaneous surface tension in a drop's life. Reproducibility of the tension data is checked to be within 5% by making measurements with the same liquid systems under the same conditions and at different times. Indeed, the surface tension of the water/air interface is measured frequently in order to check the system calibration and the cleanliness of the liquid lines. Moreover, as shown in figure 5, the measured tension values for a growing drop of a mixture of 85% glycerol and water with a viscosity of 112.9 centipoises in air show good agreement with the literature value of 66 dyne/cm (26), a result that demonstrates the capability of the technique for measuring even the surface tension at the interface between a drop of a highly viscous liquid and air during most of the drop growth process.

Figure 6 shows the instantaneous surface tension at the interface between a growing drop of a mixture of water-0.01% (by weight) Triton X-100 and air. The equilibrium value of the surface tension is 34 dyne/cm for this system (27), which is shown by a bar on the right side of figure 6. Dynamic tension measurements were made at four different liquid flow rates, ranging between 5 μ L/min and 200 μ L/min. With the surfactant adsorbing on the continuously expanding interface, the surface tension changes with time and exhibits a nonmonotonic response. The rate of interfacial dilatation, $\frac{dA}{dt}$, where A denotes the interfacial area of the drop, is relatively high at early times, as shown in figure 7. Therefore, if the rate of surfactant transport to the interface is not high enough to keep up with the rate of interface dilatation, the concentration of the surfactant on the interface, i.e. coverage per unit area, falls. The consequence of this fall in the surfactant concentration on the interface is the rise in the dynamic surface tension that is seen in figure 6. At longer times, the rate at which the interface dilatates slows as shown in figure 7: this causes the surfactant

to repopulate the interface, and the surface tension starts to fall and tends toward its equilibrium value at long times. A maximum in the value of the surface tension is attained when the lowering of the surfactant concentration on the interface due to its dilatation is just balanced by the addition of surfactant to the interface from the bulk of the drop by convection and diffusion. The results at the higher flow rates are especially striking because they display the response of the tension of the interface to the rate of interface dilatation. Similar observations of the response of dynamic surface tension to changes in rates of interfacial dilatation have also been reported by others (18, 19). It is also noteworthy that the surface tension of an interface after drop breakup is not that of a clean water/air interface: the interface that is left behind after breakup has a tension value that is close to the equilibrium value of an interface between a mixture of water-triton and air, in particular at low flow rates. This is because adsorption and equilibration of surfactant on the interface occur before the previous drop detaches, and accumulated surfactant may remain on the interface of the newly-formed drop, resulting in a low value of the surface tension at the time of zero drop age.

Figure 8 shows the variation in time of the radius of curvature and the pressure difference across the drop/air interface for the four cases shown in figure 6. In contrast to the commonly used presumption in measuring dynamic surface tension by the popular maximum bubble pressure method (12-14) and related growing drop techniques (17, 19), figure 8 makes plain that for surfactant-laden solutions, the time at which the radius of curvature is a minimum may not necessarily be the same as the time at which the pressure difference is a maximum. According to the Young-Laplace equation [6], the pressure difference across a drop's interface depends upon both the radius of curvature and the surface tension. Differentiating this expression with respect to

time yields:

$$\frac{d\Delta p}{dt} = \frac{2}{R} \frac{d\sigma}{dt} - \frac{2\sigma}{R^2} \frac{dR}{dt}. \quad [7]$$

At the instant when the drop is going through a hemispherical profile, its radius of curvature is a minimum and $\frac{dR}{dt} = 0$. Therefore, unless the surface tension attains a maximum at that instant or is independent of time — as in the case of surfactant-free solutions — so that $\frac{d\sigma}{dt} = 0$, the maximum in the pressure difference will not occur at that time. Examination of figures 6 and 8 reveals that the time at which the dynamic surface tension is a maximum does not correspond to the time at which the radius of curvature is a minimum or that at which the pressure difference is a maximum. This is not too surprising as the time for the maximum in the value of the dynamic surface tension to be attained depends solely upon the surfactant balance on the interface and not on whether the radius of curvature or the pressure difference is extremized. Therefore, in general the surface tension is changing with time when the drop becomes a hemisphere, that is $\frac{d\sigma}{dt} \neq 0$ when $\frac{dR}{dt} = 0$. This finite value of $\frac{d\sigma}{dt}$ contributes to the pressure difference and results in the time for the occurrence of the maximum in the pressure difference to lead or to lag that for the occurrence of the minimum in the radius of curvature. Further consequences of this fact are brought out in what follows.

The strong dependence of the dynamic behavior of surface tension on the transport rate of the surfactant is further reinforced by the results of figure 9, which shows the evolution in time of the instantaneous surface tension of a mixture of water and Triton X-100 at various bulk concentrations. In this figure, the tension results shown are from three runs made at the same liquid flow rate of $10 \mu\text{L}/\text{min}$. As the bulk concentration increases, the average of the measured values of the surface tension decreases, a result that accords with intuition. Moreover, as the bulk concentration increases, the gradient of the surfactant concentration between the bulk of the drop and its interface increases: this accelerates the transport of the surfactant to the interface by diffusion

and, therefore, shifts the occurrence of the maximum in the surface tension to earlier times. With the slower rate of transport of the surfactant in the less concentrated solutions, the surface tension of these dilute solutions rise to higher values from their equilibrium values in comparison to more concentrated solutions, a result the basis for which is also apparent from the trend in the measurements at high flow rates reported in figure 6.

The nonmonotonic behavior in time of the dynamic surface tension as measured by the growing drop technique of course occurs with other surfactant-laden solutions. Figure 10 shows the evolution in time of the instantaneous surface tension at the interface between a growing drop of a mixture of water-6 mM Sodium Dodecyl Sulphate (SDS), a highly active surfactant, and air. Owing to the fast rate of transport of this surfactant, the measured surface tension displays rapid changes either early during its rise or later during its fall, and rapidly tends to its equilibrium value of 46.1 dyne/cm (28). Moreover, the maximum in the dynamic surface tension of the SDS solution occurs during the pre-hemisphere period as a result of the rapid transport of this surfactant. The latter result stands in contrast to solutions with slowly transporting surfactants, like Triton X-100 shown in figure 6. This discovery remedies the earlier measurements of drops containing SDS with a similar technique (19), where the nonmonotonic behavior and, in particular, the maximum of the surface tension were not detected because the equipment used in (19) was not fast enough to make measurements during the pre-hemisphere period of drop growth. Otherwise, the present results of the dynamic surface tension in the post-hemisphere period of the drop growth are in good agreement with those reported in (19), which provides yet another check of the validity of the present method.

Figures 11 and 12 show the evolution in time of the instantaneous surface tension of two aqueous solutions with low activity surfactants, 0.01% (by weight) Sodium Dioctyl

Sulfosuccinate and 0.01% (by weight) Induce AL-2700. As the rate of interfacial dilatation greatly exceeds the rate of transport of the surfactant in the early period of drop growth, a relatively "clean" interface is generated when the surface tension is extremized. This results in the maximum values of the dynamic surface tension approaching the tension of the pure solvent (distilled water). Thereafter, a long time is taken for the tension to reach its equilibrium value. For the Sodium Dioctyl Sulfosuccinate solution, a slow rearrangement of equilibrated surfactant molecules on the interface occurs, resulting in a large departure of the measured surface tension from its equilibrium value at long time as shown in figure 11. Evidently, extrapolation from dynamic tension measurements to the equilibrium tension in such systems, as suggested in (29), is inappropriate. In figures 11 and 12, the equilibrium value of the surface tension for the 0.01% solution of Sodium Dioctyl Sulfosuccinate of 35.3 dyne/cm is given in the literature (28), and that for the 0.01% solution of Induce of 38.9 dyne/cm was measured with a technique based on the pendant drop method in our laboratory (30).

4.2. Oscillations of newly-formed drops

Oscillations can occur when a new drop forms, following the detachment of the previous drop and the rebound of the liquid that is left behind. During the period of drop oscillations, uncertainties in the drop shape and pressure render the direct determination of the surface tension by the present technique impossible unless a comprehensive understanding of the complex hydrodynamics inside the growing drop is developed (21, 22). However, our observations provide for the first time visual evidence of occurrence, evolution, and disappearance of the oscillations and clarification of the effects of these oscillations on surface tension measurements.

Figure 13 shows a series of photographs that illustrate the early stages in the for-

mation of a water drop into air at a liquid flow rate $Q = 100\mu\text{L}/\text{min}$. Immediately after the previous drop detaches (figure 13(a)), the liquid left behind in the throat rebounds toward the capillary with great acceleration owing to the unbalanced force of surface tension (31) and collides with the downflowing liquid in the pipe. Under the impact of this rebound and collision, the new drop that is forming at the end of the capillary looks as shown in figure 13(b) 0.5 millisecond later. The liquid rebound and impact excite oscillations on the surface of the newly-formed drop. A half of a period of oscillation is depicted in going from figure 13(c) to (d), where a drop whose bottom is visibly flattened 1 millisecond after detachment is shown in figure 13(c) and the same drop whose tip is visibly elongated 1 millisecond later is shown in figure 13(d). Oscillations of the drop interface continue with gradually decreasing amplitude and frequency due to viscous damping and increasing drop volume (cf. (11)), as illustrated in figures 13(e)-(i). After approximately 28 milliseconds have elapsed (figure 13(j)), the oscillations are completely damped out and the drop begins to grow stably as a section of a shape.

As the drop interface, the pressure inside the drop too oscillates during the early times of drop formation. Figure 14 shows the oscillations of the pressure inside a water drop growing in air at liquid flow rates of $Q = 100\mu\text{L}/\text{min}$ and $10\mu\text{L}/\text{min}$. The solid lines in figure 14 are results calculated from the Young-Laplace formula [6] with a constant surface tension of 73 dyne/cm. Since the drop volume at zero time is nonzero and composed of a combination of the rebounding liquid and the dowflowing liquid in the pipe, a finite initial pressure difference across the drop interface is established. Plainly, the pressure rises and falls dramatically inside the newly formed drop, in concert with the oscillations of the drop interface. The amplitude and frequency of the pressure oscillations decrease rapidly and the pressure begins to vary stably as predicted by [6] after 30 milliseconds.

It is well known that the damping of drop oscillations is a function of the properties of the drop and ambient fluids, in particular of viscosities. For high viscosity fluids, the oscillations of millimeter-sized drops can be damped out within a few milliseconds or less or the motion can be nonoscillatory (11). This fact is demonstrated in figure 15 by our experimental results for a drop of a mixture of 70% (by weight) glycerol and water with a viscosity of 22.9 centipoises and a surface tension of 69.3 dyne/cm (26) growing in air. Indeed, oscillations of the drop interface and pressure cannot be observed even within one millisecond after the previous drop detaches: both the drop shape and the pressure field evolve aperiodically in time to their forms that are consistent with those of a drop growing as a section of a sphere. Figure 15 shows that the pressure difference for the high viscosity drop starts at a very low value and increases monotonically until approaching that predicted by [6] after about 30 milliseconds. The departure of the measured initial pressure difference from that predicted by [6] is experimentally found to increase and last longer as the viscosity of the drop fluid increases. The peculiar behavior of the pressure inside highly viscous drops can affect the values of the surface tension measured at short times and, therefore, warrants further attention. This is a point to which we return in the next subsection. However, it has also been found that drops of surfactant-laden solutions experience relatively shorter times of oscillations because the surfactant adsorbed on the interface stagnates the interface and, therefore, increases the damping of the oscillations.

4.3. Effect of viscosity

The effect of viscosity on surface tension measurements made by the growing drop technique has heretofore not been explored (cf. (19)). To carry out a systematic investigation of the effect of viscosity, glycerol-water solutions containing different amounts of glycerol by weight were prepared and drops of these solutions were formed

from the capillary at two different flow rates. The viscosities and surface tensions of these solutions are: (a) $\mu = 6.0$ centipoises, $\sigma = 71.1$ dyne/cm for the 50% glycerol-water solution, (b) $\mu = 22.9$ centipoises, $\sigma = 69.3$ dyne/cm for the 70% glycerol-water solution, and (c) $\mu = 112.8$ centipoises, $\sigma = 66.0$ dyne/cm for the 85% glycerol-water solution (26). Figure 16 shows that at short times, the surface tension as determined by the Young-Laplace formula [6] can be substantially lower than the actual value of the surface tension. Figure 16 makes plain that the discrepancy between the measured and expected values of surface tension increases as drop viscosity increases. To account for this viscous effect, it is at first sight plausible to estimate the viscous contributions to the normal stress balance by assuming that the flow inside the growing drop is radial flow. Unfortunately, the viscous corrections made in this manner can be shown to affect the values of the dynamic surface tension by no more than 2%.

5. CONCLUDING REMARKS

According to the foregoing results, the growing drop technique is a simple, accurate, and reliable method for determining the evolution in time of the dynamic surface tension of a *single* interface between a complex-mixture liquid drop and air on time scales as early as 20 milliseconds. This is an improvement over related growing drop techniques, e.g. that described in [19], where the earliest times of tension measurement range between 40 and 70 milliseconds. However, in contrast to the growing technique as practiced in [19] and elsewhere, the new technique is, in principle, capable of making measurements in as short as 1/6 of a millisecond of surface age. By using the unique experimental tools available in this work, insights are also provided here for the first time into why the growing drop technique as practiced currently is not capable of furnishing dynamic surface tension data when $1/6 < t < 20$ milliseconds.

Underdamped oscillations in the case of low viscosity systems and aperiodic decay in the case of high viscosity systems of the drop interface and pressure render interpretation of tension measurements impossible at these early times with the simple but easy to use static Young-Laplace formula [6]. Because oscillations on the surface of a liquid drop forming into another liquid would be damped out more quickly than those on the surface of a liquid drop forming into a gas (32), the growing drop technique as it stands should be able to determine the evolution of dynamic surface tension in liquid-liquid systems starting at earlier times than in liquid-gas systems.

Because a maximum in the surface tension is attained when the lowering of the surfactant concentration on the interface due to its dilatation is just balanced by the addition of fresh surfactant to it from the drop bulk by convection and diffusion, it is demonstrated in this work that surface tension, pressure, and radius of curvature of the drop may not all be extremized at the same instant in time. This finding has ramifications for the popular maximum bubble pressure method (12-14) and other growing drop techniques (17, 19).

A systematic investigation of the effect of drop viscosity has revealed that increasing viscosity results in an underestimation of the surface tension by the Young-Laplace formula at small times. However, tension measurements are insignificantly affected by viscosity for times exceeding about 100 milliseconds. At times earlier than 100 milliseconds, however, the assumption of radial flow inside the drop is unable to account for the magnitude of the viscous stresses and thus cannot provide the viscous correction needed to produce correct values of the instantaneous tension.

The growing drop technique is also an important tool to study convection/diffusion and kinetics of adsorption/desorption of surfactants to and from moving interfaces. Theoretical analysis of this problem requires knowledge of the flow inside the drop. MacLeod and Radke (33) have studied this problem under the assumption that the

flow inside the drop is purely radial flow. Recent calculations, however, indicate that the radial flow assumption may not always hold (22).

Therefore, there is a need to better understand the dynamics of drop formation. Computational techniques based on the finite element (11, 21, 22) and boundary element methods (34) can be used to compute rigorously the transient profiles of growing drops and flow fields inside them. By means of such computations, the early times after zero surface age, the effects of viscosity, and the validity of the radial flow assumption can all be examined in detail. With the aid of rigorous computations, one ought to be able to back out the dynamic surface tension without reliance on the simple but limited Young-Laplace formula. More careful flow visualization experiments than those carried out to date (see, e.g., (31, 35, 36)) are also needed to complement the computations and, in particular, to gain insights into the physics of drop formation during the first few milliseconds after drop breakup. Furthermore, the new computational and experimental studies should emphasize not only liquid-gas systems as in this work but liquid-liquid systems (cf. (18, 19)) as well because of the importance of the latter systems in chemical, petrochemical, and pharmaceutical industries.

Acknowledgements

This work was supported by the Spray Drift Task Force and the Divisions of Chemical Sciences (O.A. Basaran), Material Sciences (M.T. Harris), and Advanced Energy Projects (M.T. Harris), Office of Basic Energy Sciences, U.S. Department of Energy under contract DE-AC05-84OR21400 with Martin Marietta Energy Systems, Inc. The authors thank Dr. C. Hermansky, Professor C. J. Radke, and C. A. MacLeod for their valuable comments and suggestions throughout this research, and for continuing stimulating discussions on dynamic surface tension. We are also indebted to our colleagues in the ViSCLab at the Oak Ridge National Laboratory for their invaluable assistance

in the preparation of the photographs.

REFERENCES

1. Clift, R., Grace, J.R., and Weber, M.E., *Bubbles, Drops, and Particles*. Academic Press, New York, 1978.
2. Edwards, D.A., Brenner, H., and Wasan, D.T., *Interfacial Transport Processes and Rheology*. Butterworth-Heinemann, Boston, 1991.
3. Djabbarah, H.F. and Wasan, D.T., *Chem. Eng. Sci.* **37**, 175 (1982).
4. Lucassen, J. and van den Tempel, M., *J. Colloid Interface Sci.* **41**, 491 (1972).
5. Hard, S. and Neumann, R.D., *J. Colloid Interface Sci.* **83**, 315 (1981).
6. Somasundaran, P., Danitz, M., and Mysels, K.J., *J. Colloid Interface Sci.* **48**, 410 (1974).
7. Lunkenheimer, K. Hartenstein, C., Miller, R. and Wantke, K.D., *Colloids and Surfaces* **8**, 271 (1984).
8. Caskey, J.A. and Barlage, Jr. W.B., *J. Colloid Interface Sci.* **35**, 46 (1971).
9. Thomas, W.D.E. and Potter, L., *J. Colloid Interface Sci.* **50**, 397 (1975).
10. Bohr, N., *Phil. Trans. A* **209**, 281 (1909).
11. Basaran, O.A., *J. Fluid Mech.* **241**, 169 (1992).
12. Mysels, K.J., *Langmuir* **2**, 428 (1986).
13. Hua, X.Y. and Rosen, M.J., *J. Colloid Interface Sci.* **2**, 652 (1988).
14. Garrett, P.R. and Ward, D.R., *J. Colloid Interface Sci.* **132**, 475 (1989).
15. Pierson, F.W. and Whitaker S., *J. Colloid Interface Sci.* **54**, 203 (1976).
16. Henderson, D.C. and Micale, F.J., *J. Colloid Interface Sci.* **158**, 289 (1993).
17. Passerone, A., Liggieri, L., Rando, N., Ravera, F., and Ricci, E., *J. Colloid Interface Sci.* **146**, 152 (1991).
18. Nagarajan, R. and Wasan, D.T., *J. Colloid Interface Sci.* **159**, 164 (1993).
19. Macleod, C.A. and Radke, C.J., *J. Colloid Interface Sci.* **160**, 435 (1993).

20. Michael, D.H., *Ann. Rev. Fluid. Mech.* **13**, 189 (1981).
21. Basaran, O.A., Zhang, X., and Harris, M.T., Paper 51k, presented at the 1993 Winter Annual Meeting of the AIChE, St. Louis, Missouri.
22. Basaran, O.A., Zhang, X., and Harris, M.T., in preparation.
23. Liggieri, L., Ravera, F., and Passerone, A., *J. Colloid Interface Sci.* **140**, 436 (1990).
24. Davies, J.T. and Rideal, E.K., *Interfacial Phenomena*. Academic Press Inc., Boston, 1961.
25. Timmermans, J., *The Physico-Chemical Constants of Binary Systems in Concentrated Solutions, Vol. 4*. Interscience Publishers, New York, 1960.
26. Hodgman, C.D., *Handbook of Chemistry and Physics*. Chemical Rubber Publishing Co., Ohio 1951.
27. Lin, S.Y., McKeigue, K., and Maldarelli, C., *AICHE J.* **36**, 1785 (1990).
28. Mysels, K.J., *Langmuir* **2**, 423 (1986).
29. Serrien, G. and Joos, P., *J. Colloid Interface Sci.* **139**, 149 (1990).
30. Harris, M.T. and Byers, C. H., *An Advanced Technique for Interfacial Tension Measurement in Liquid-Liquid Systems*. ORNL/TM-10734 (1989).
31. Peregrine, D.H., Shokes, G., and Symon, A., *J. Fluid Mech.* **212**, 25 (1990).
32. Miller, C.A. and Scriven, L.E., *J. Fluid Mech.* **32**, 417 (1968).
33. MacLeod, C.C. and Radke, C.J., submitted to *J. Colloid Interface Sci.* (1993).
34. Wong, H., Rumschitzki, D., and Maldreli, C., Paper 36g, presented at the 1993 Winter Annual Meeting of the AIChE, St. Louis, Missouri.
35. Humphrey, J.A.C., Hummel, R.L., and Smith, J.W., *Chem. Eng. Sci.* **29**, 1496 (1974).
36. Johnson, G. and Marschall, E., *Int. J. Multiphase Flow* **12**, 127 (1986).

Figure Captions

Figure 1. Sequences of drop shapes (I-III) during formation or growth of a drop from a capillary. As the drop grows, the pressure difference across the drop interface and the radius of curvature of the drop vary in time as shown.

Figure 2. Time rate of change of the radius of curvature of a growing drop dR/dt normalized by the radius of curvature R at various flow rates. The drop is assumed to grow as a spherical section and the abscissa has been made dimensionless by dividing the actual time by the time it takes the drop to take on a hemispherical shape.

Figure 3. Experimental setup for measuring the dynamic surface tension of the interface between a growing drop and an ambient fluid.

Figure 4. Time sequence of shapes of forming or growing drops observed in experiments: (a) necking of drop, (b) rupture of neck or throat, (c) oscillations of newly-formed drop, (d) pre-hemispherical drop, (e) hemispherical drop, and (d) post-hemispherical drop.

Figure 5. Surface tension of the interface between growing drops of triple distilled water, top, water plus glycerol, middle, and water plus propanol, bottom, and air at different liquid flow rates. Points correspond to the actual dynamic surface tension measurements and the solid lines are the equilibrium values of the surface tension.

Figure 6. Surface tension of the interface between a growing drop of water plus 0.01% Triton X-100 and air at different liquid flow rates. Points correspond to the actual dynamic surface tension measurements and the bar on the right side is the equilibrium value of the surface tension.

Figure 7. Interfacial dilatation rate of a growing drop $\frac{1}{A} \frac{dA}{dt}$ at various flow rates. The drop is assumed to grow as a spherical section and the abscissa has been made dimensionless by dividing the actual time by the time it takes the drop to take on a hemispherical shape.

Figure 8. Radius of curvature and pressure difference of a drop of water plus 0.01% Triton X-100 growing out of a capillary into air at various flow rates.

Figure 9. Surface tension of the interface between water plus Triton X-100 and air at different Triton concentrations. The liquid flow rate is held fixed at $Q = 10\mu\text{L}/\text{min}$.

Figure 10. Surface tension of the interface between a growing drop of water plus 6 mM Sodium Dodecyl Sulfate (SDS) and air at different liquid flow rates. Points correspond to the actual dynamic tension measurements and the bar on the right side is the equilibrium value of the surface tension.

Figure 11. Surface tension of the interface between a growing drop of water plus 0.01% Sodium Dioctyl Sulfosuccinate and air at different liquid flow rates. Points correspond to the actual dynamic tension measurements and the bar on the right side is the equilibrium value of the surface tension.

Figure 12. Surface tension of the interface between a growing drop of water plus 0.01% Induce AL-2700 and air at different liquid flow rates. Points correspond to the actual dynamic tension measurements and the bar on the right side is the equilibrium value of the surface tension.

Figure 13. Experimental observations of oscillations of a newly-formed water drop in air at a liquid flow rate $Q = 100\mu\text{L}/\text{min}$.

Figure 14. Instantaneous pressure difference across the interface between a growing drop of water and air at different liquid flow rates. Points correspond to the actual pressure measurements and the solid lines are the theoretical predictions based on the Young-Laplace formula.

Figure 15. Instantaneous pressure difference across the interface between a growing drop of water plus 70% glycerol and air at different liquid flow rates. Points correspond to the actual pressure measurements and the solid lines are the theoretical predictions based on the Young-Laplace formula.

Figure 16. Surface tension of the interface between a growing drop of water plus different amounts by weight of glycerol and air at two different flow rates. Points correspond to the actual dynamic surface tension measurements and the solid lines to the equilibrium values of the surface tension.

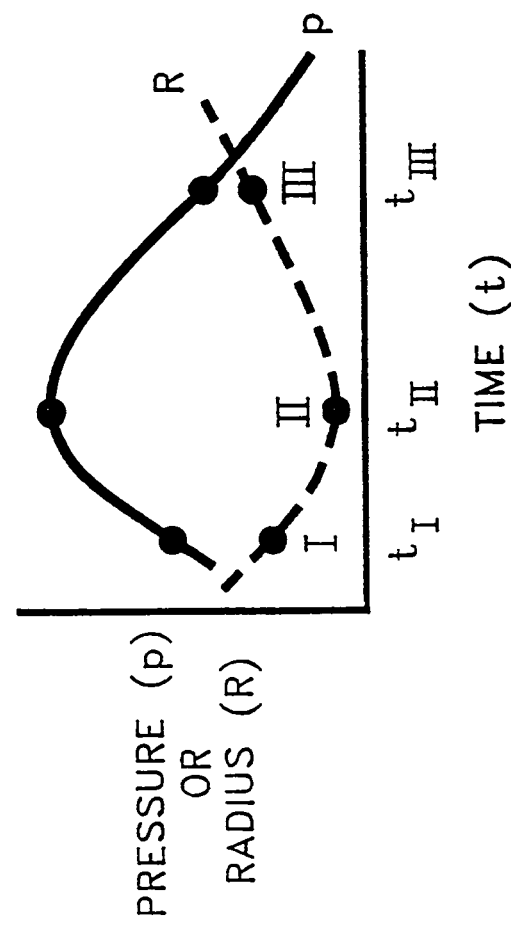
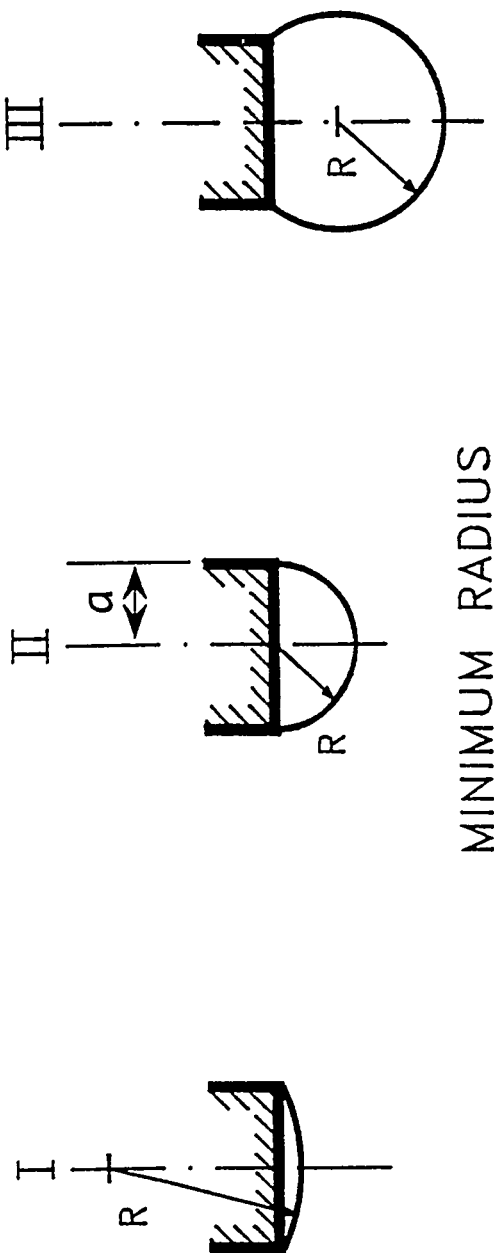


Figure 1. Zhang *et al.*

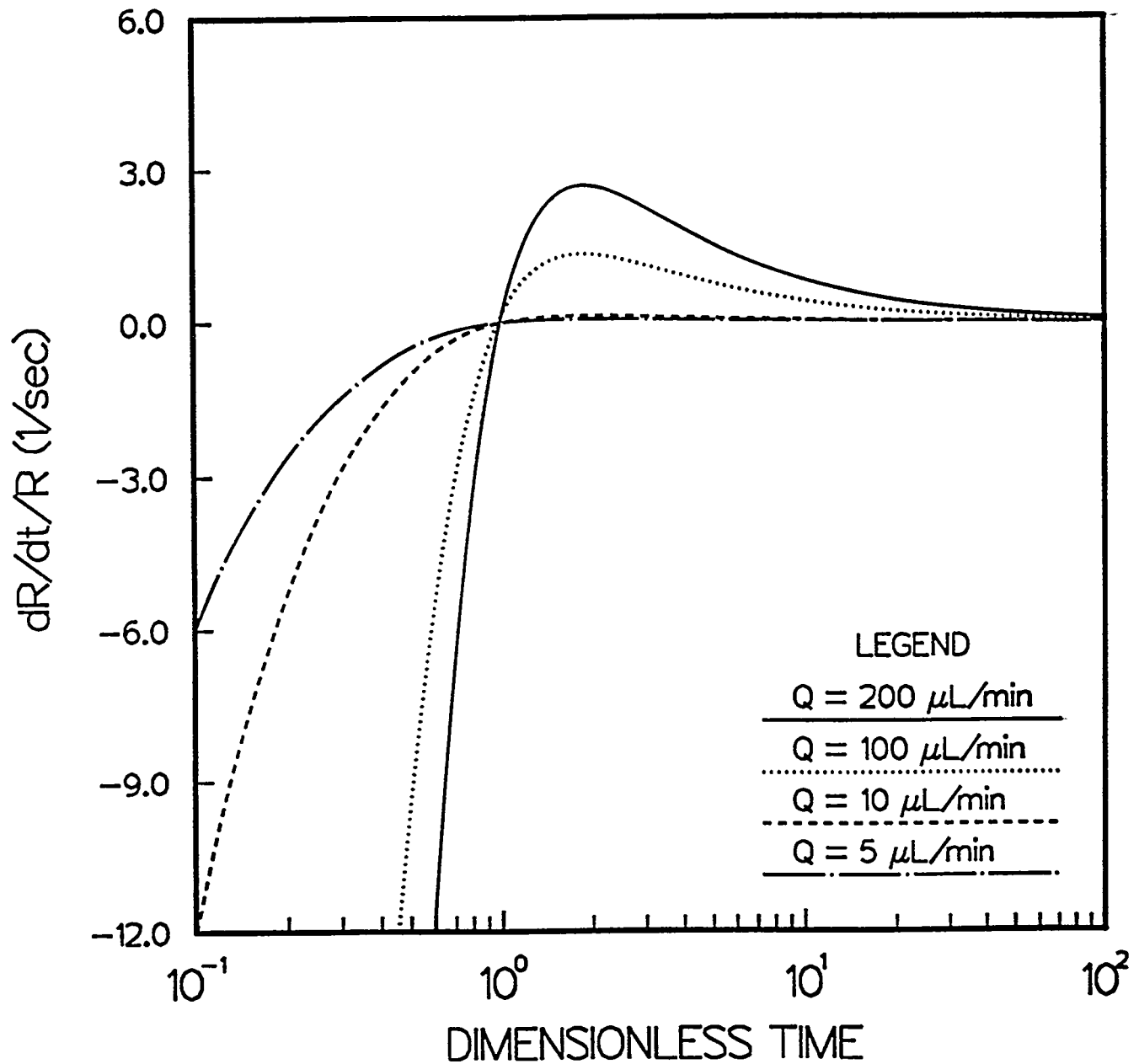


Figure 2. Zhang *et al.*

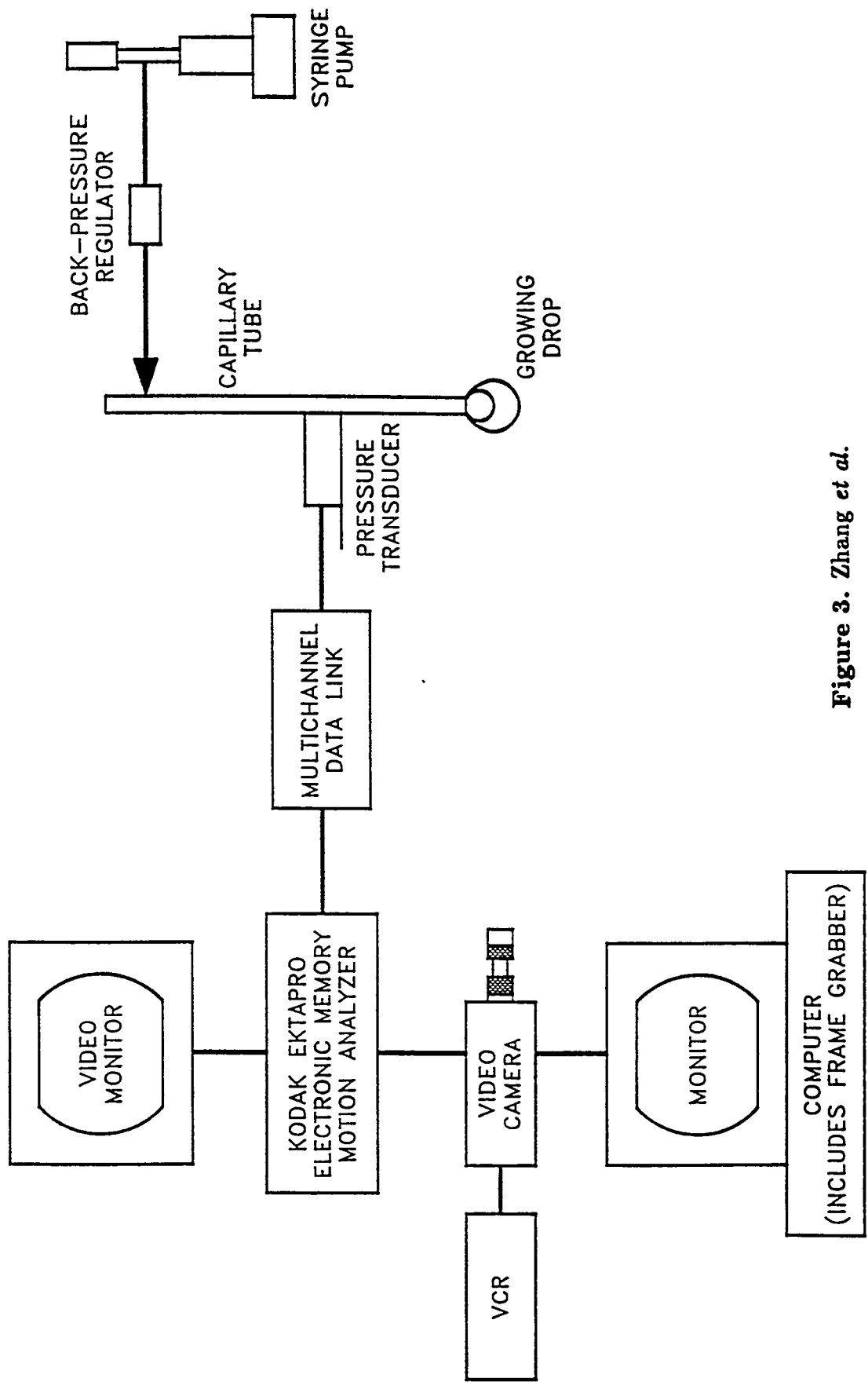


Figure 3. Zhang *et al.*

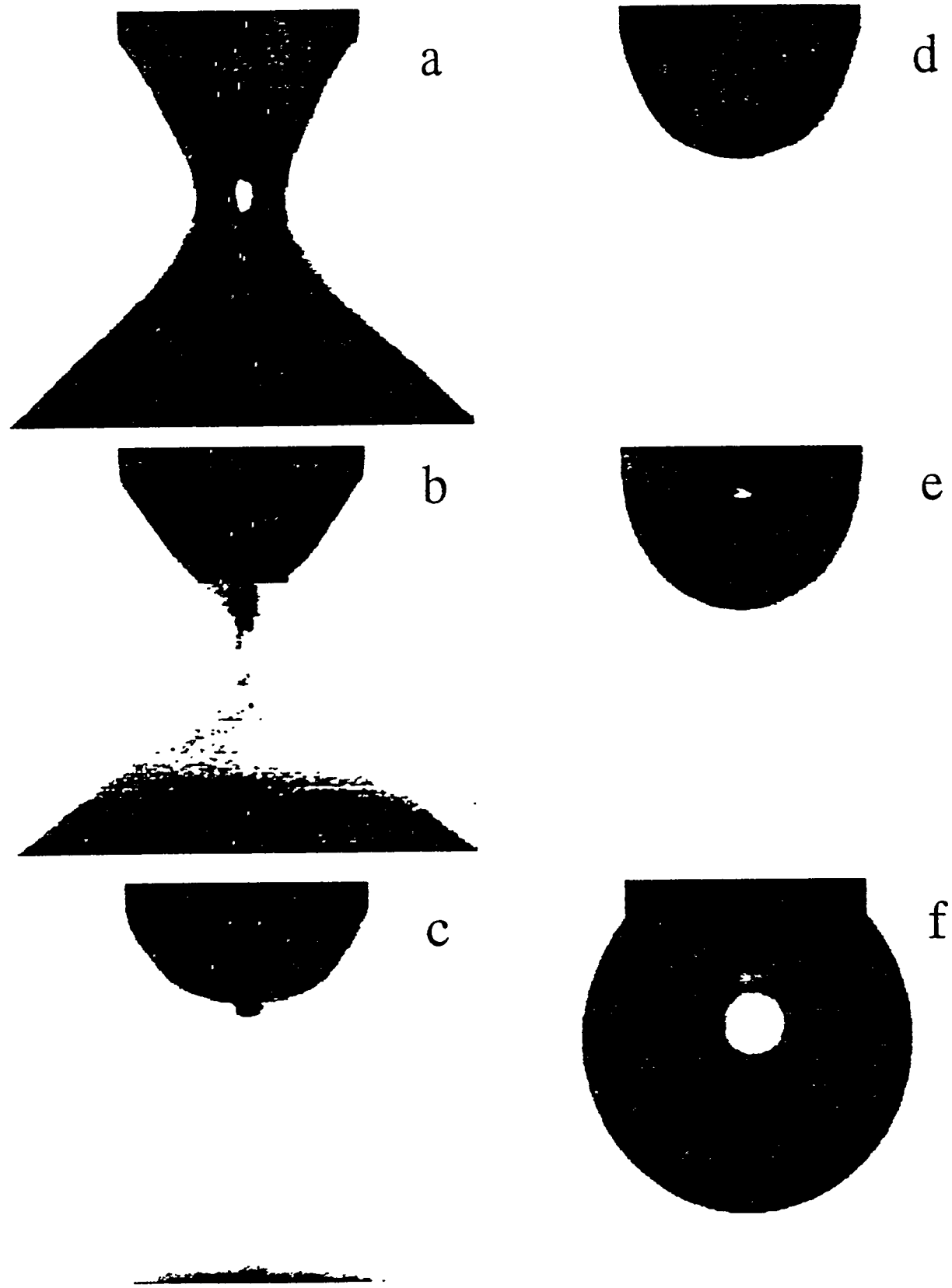


Figure 4. Zhang *et al.*

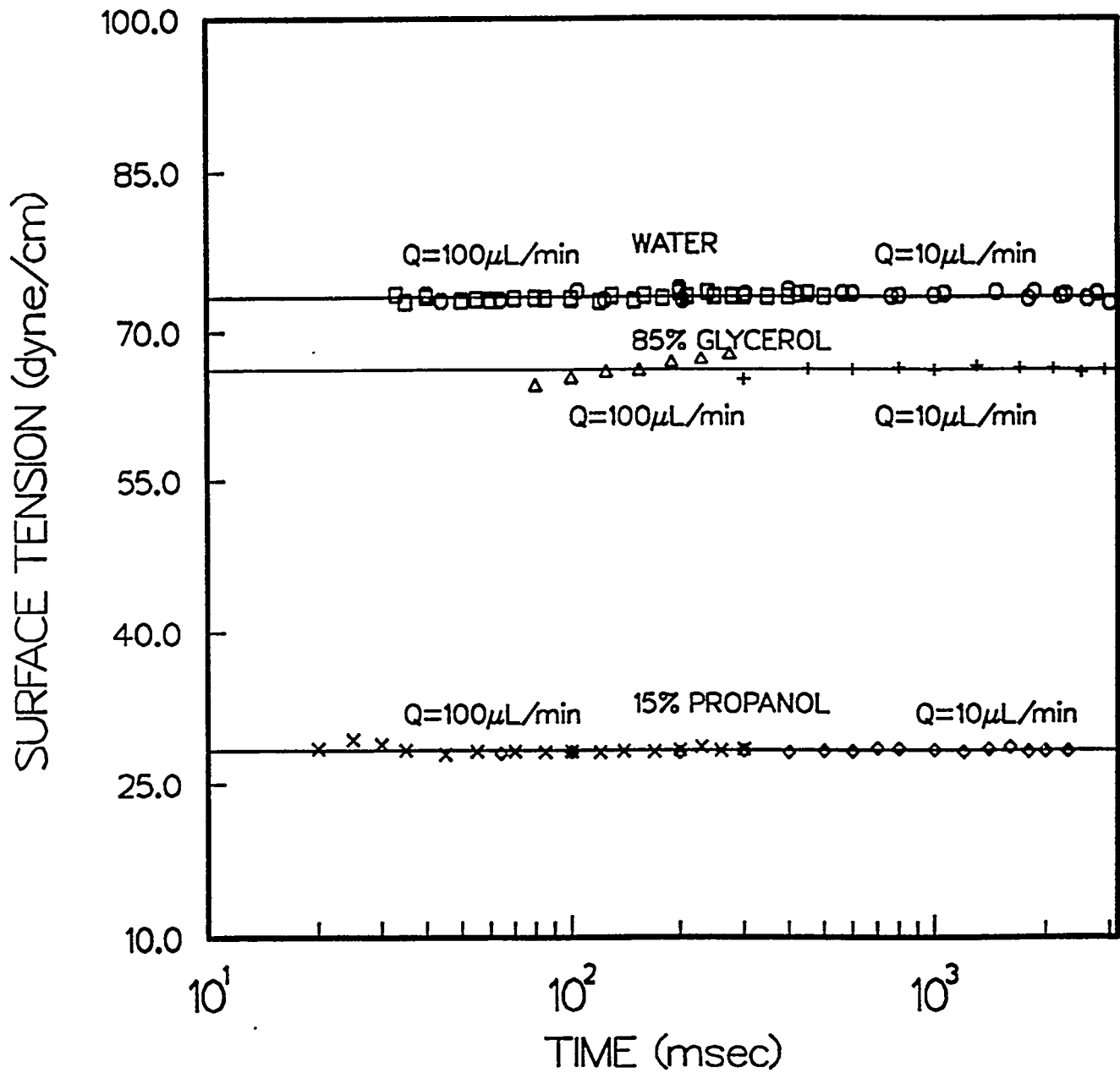


Figure 5. Zhang *et al.*

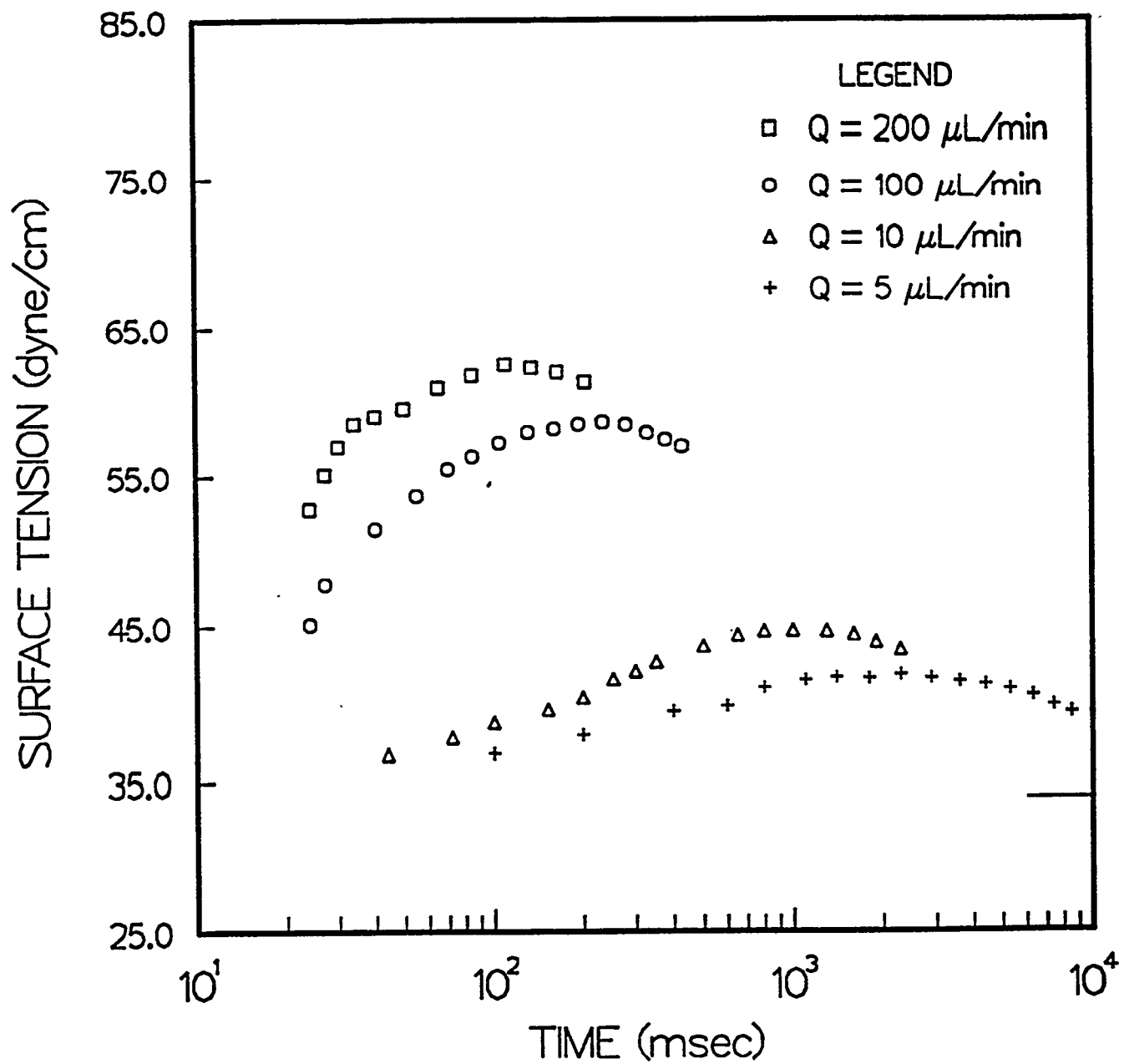


Figure 6. Zhang *et al.*

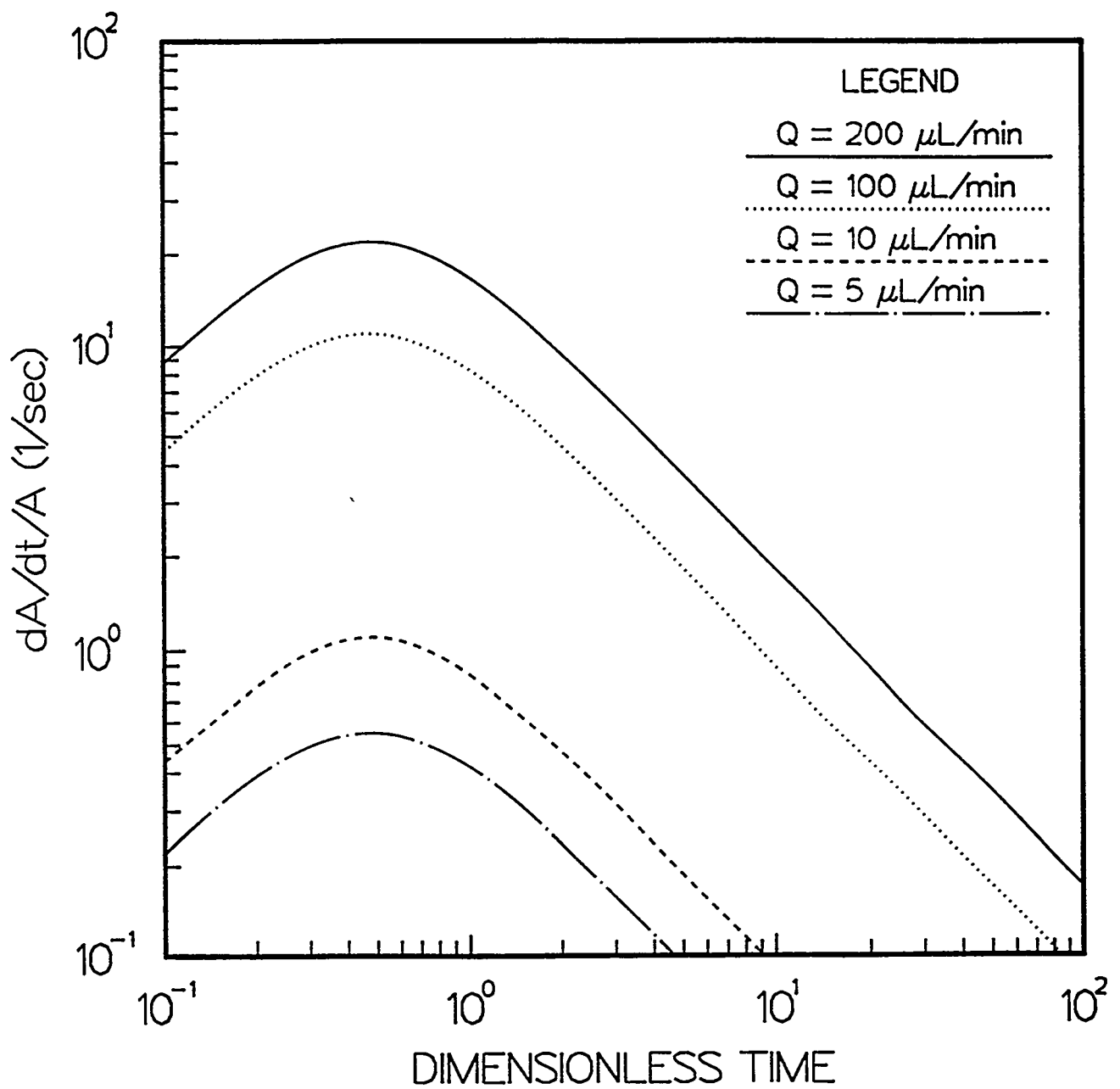


Figure 7. Zhang *et al.*

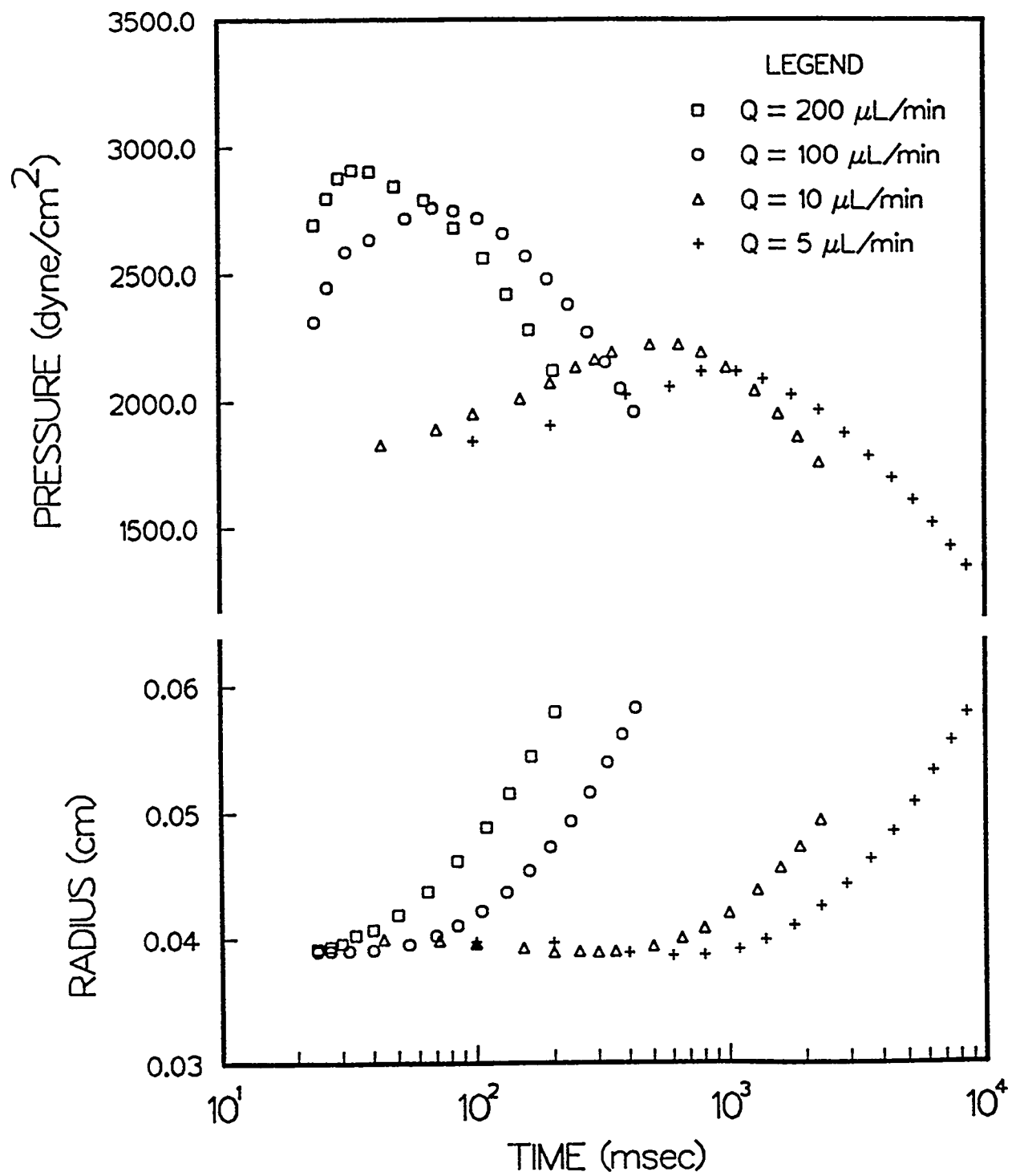


Figure 8. Zhang *et al.*

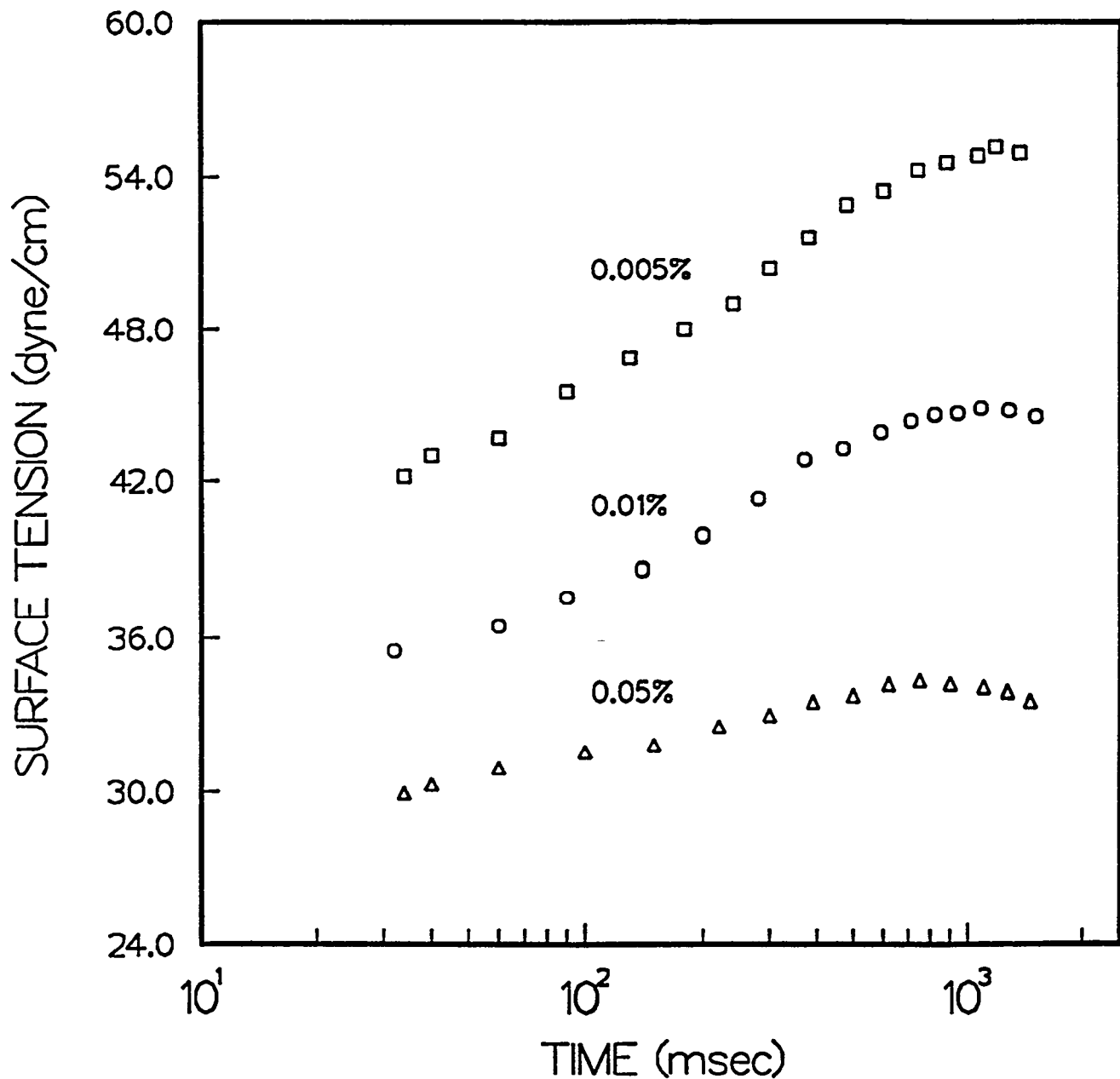


Figure 9. Zhang *et al.*

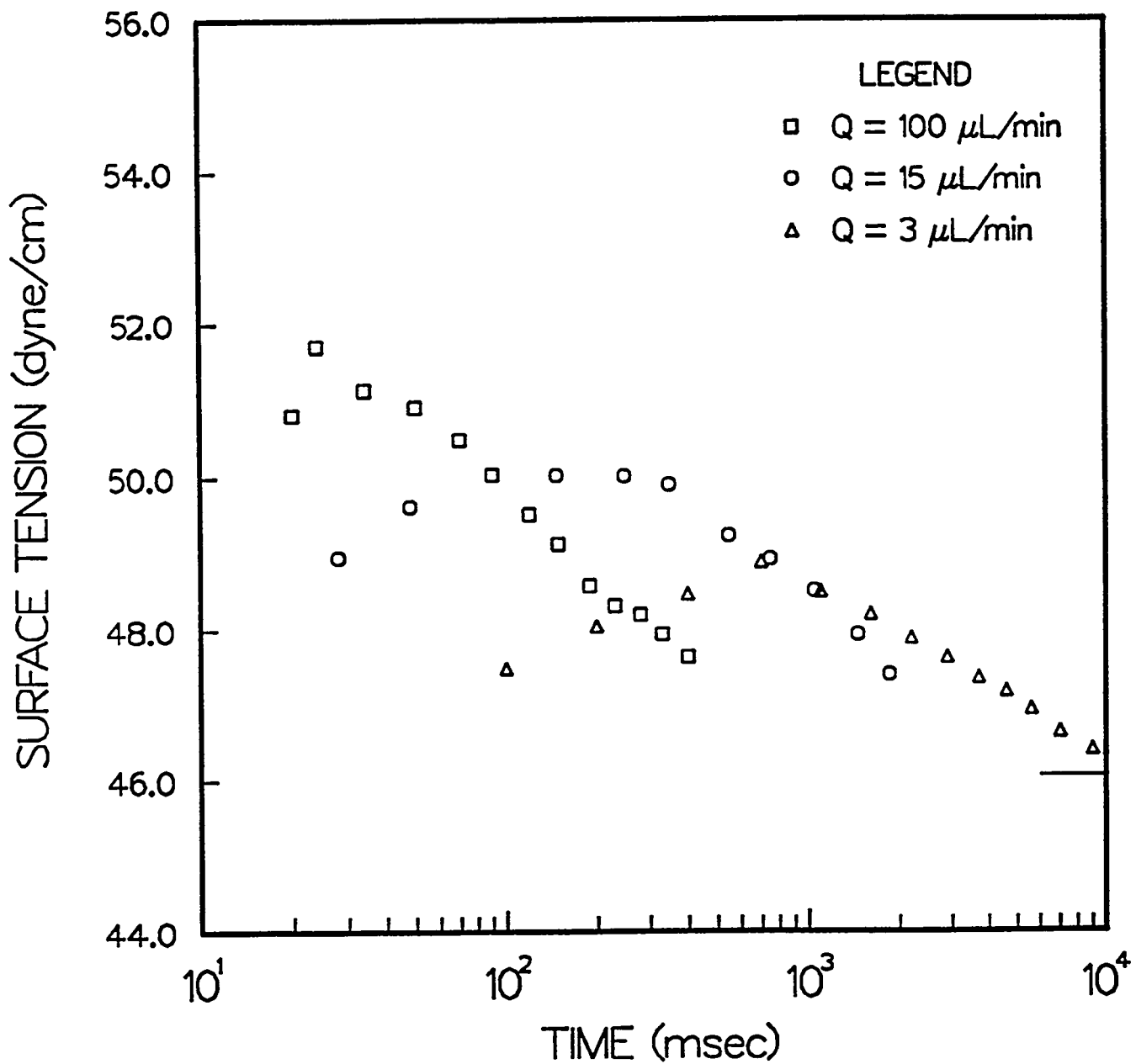


Figure 10. Zhang *et al.*

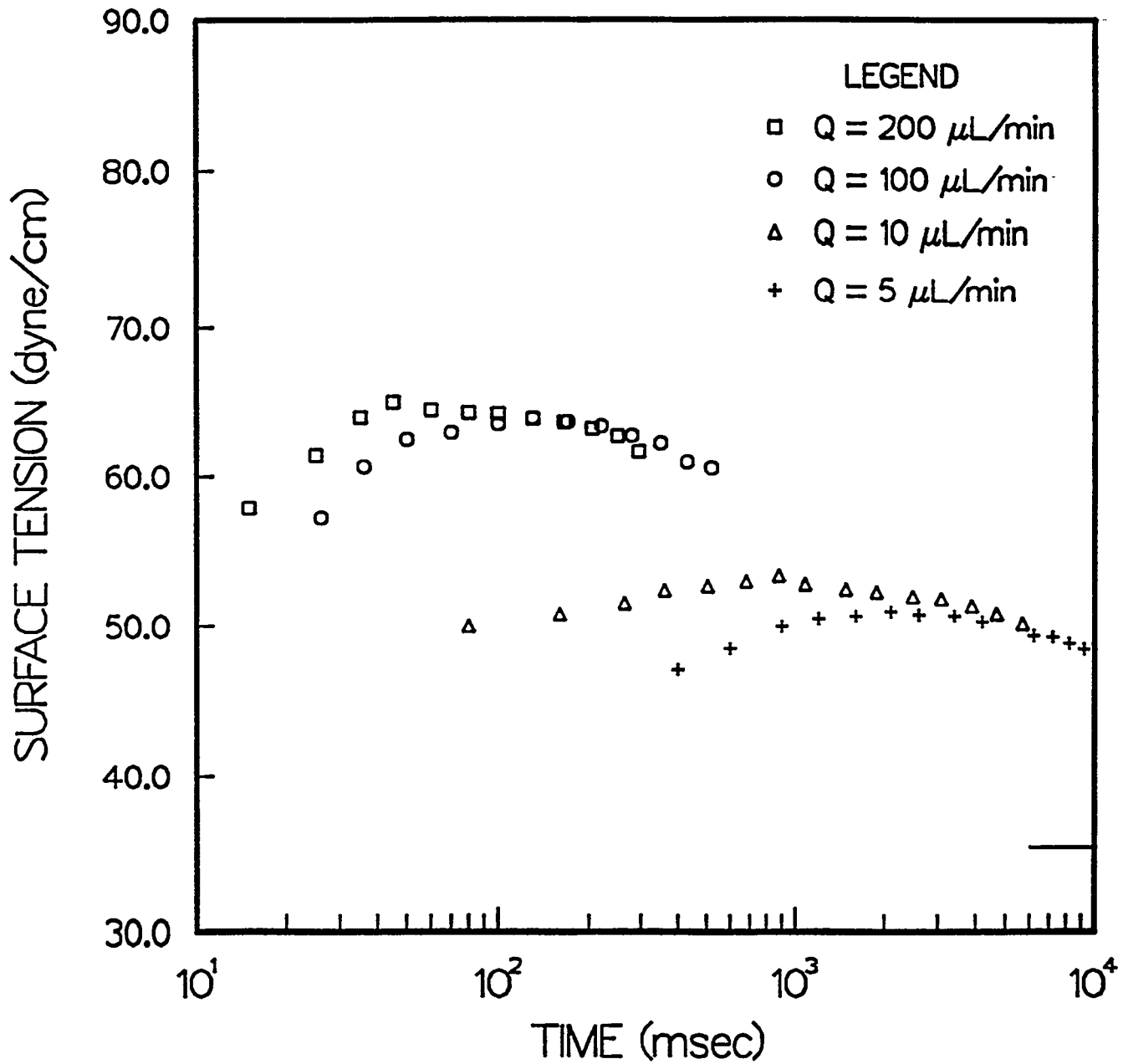


Figure 11. Zhang *et al.*

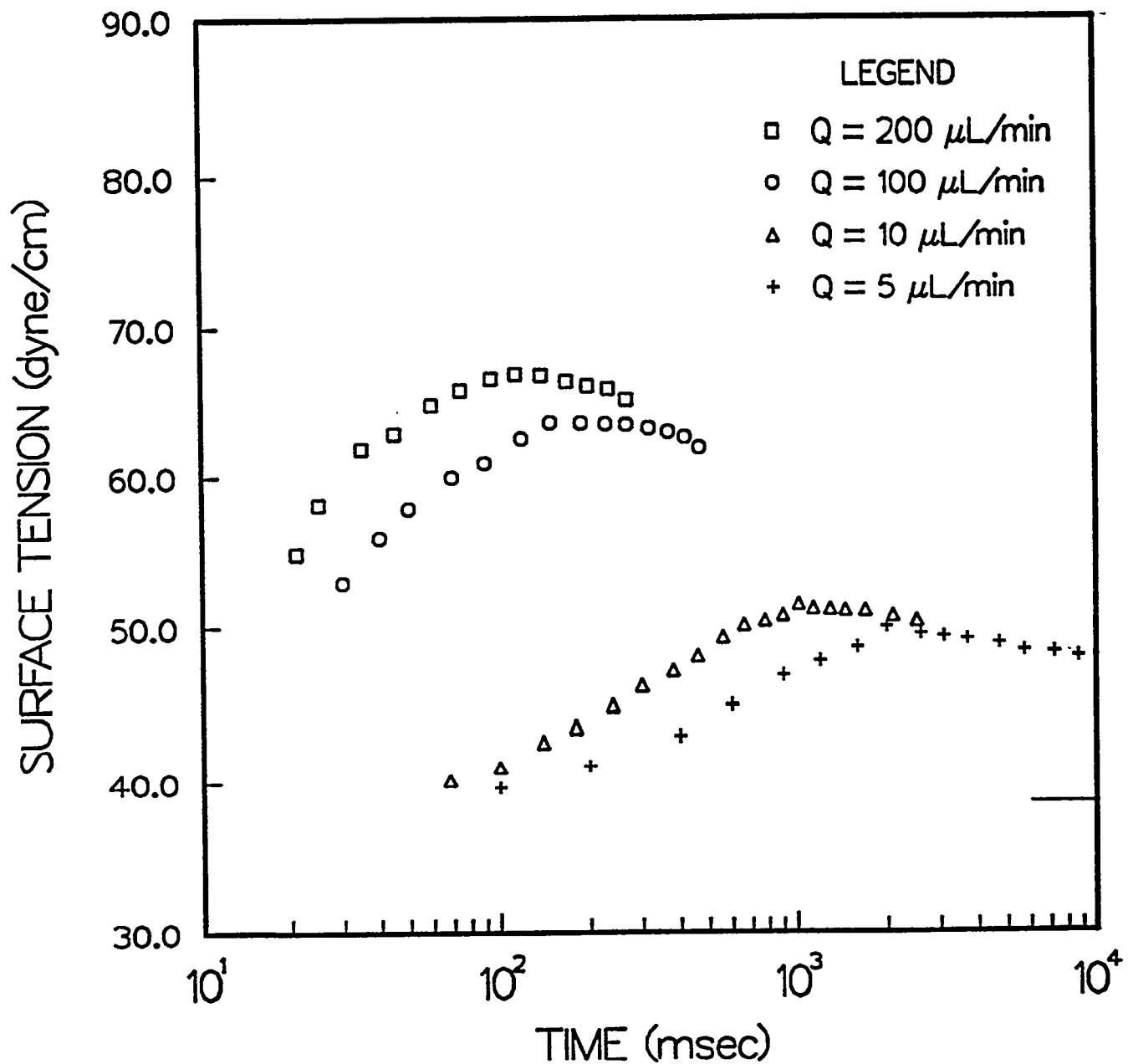


Figure 12. Zhang *et al.*



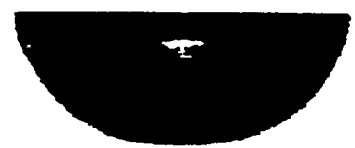
a



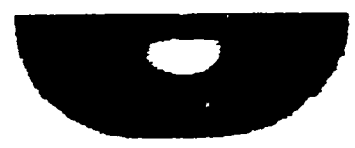
b



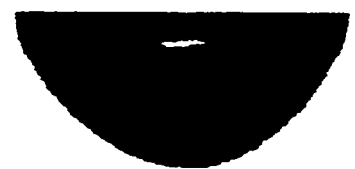
f



g



c



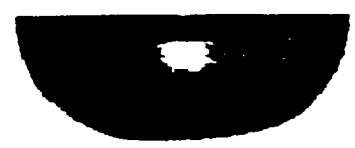
h



d



i



e



j

Figure 13. Zhang *et al.*

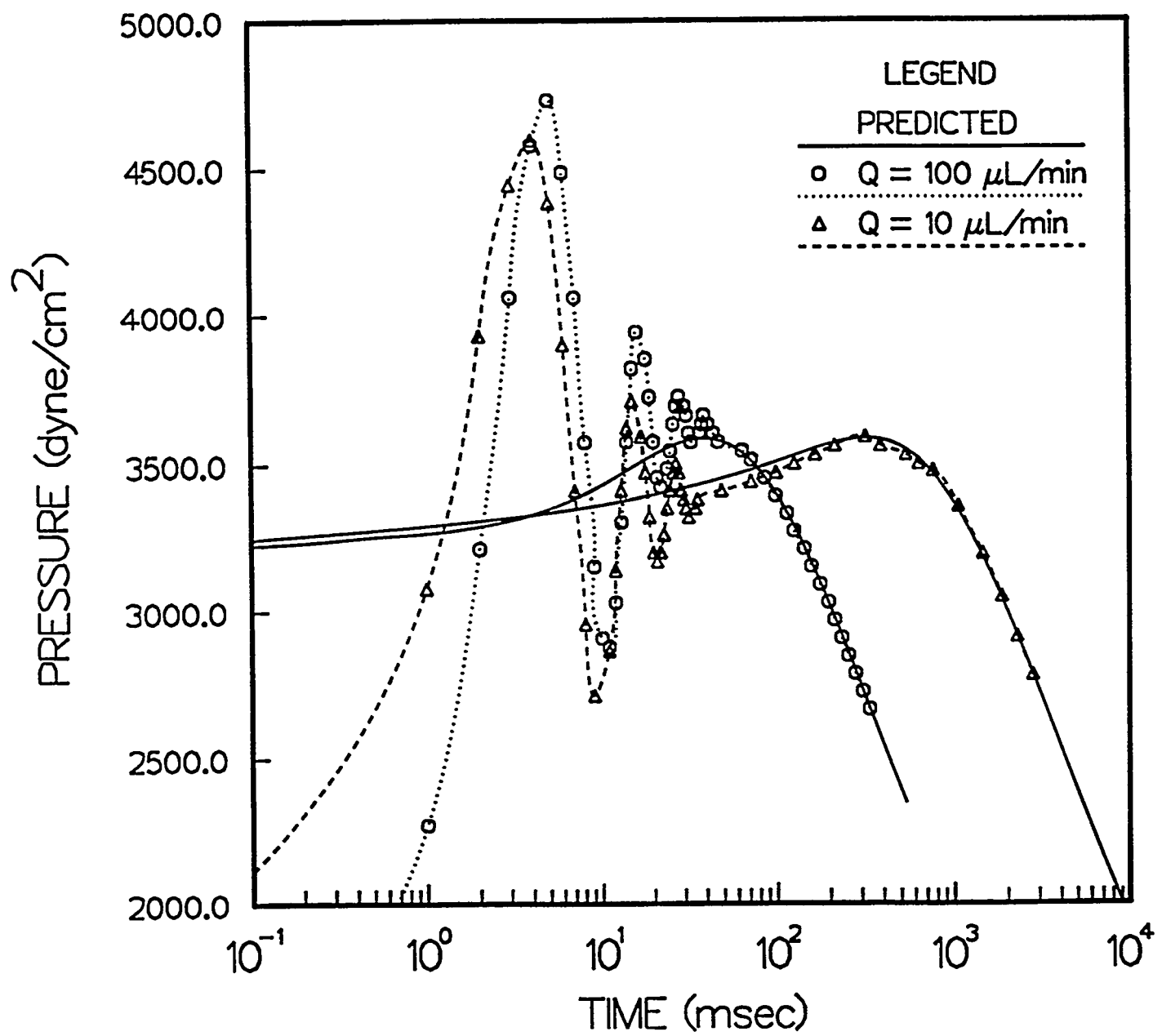


Figure 14. Zhang *et al.*

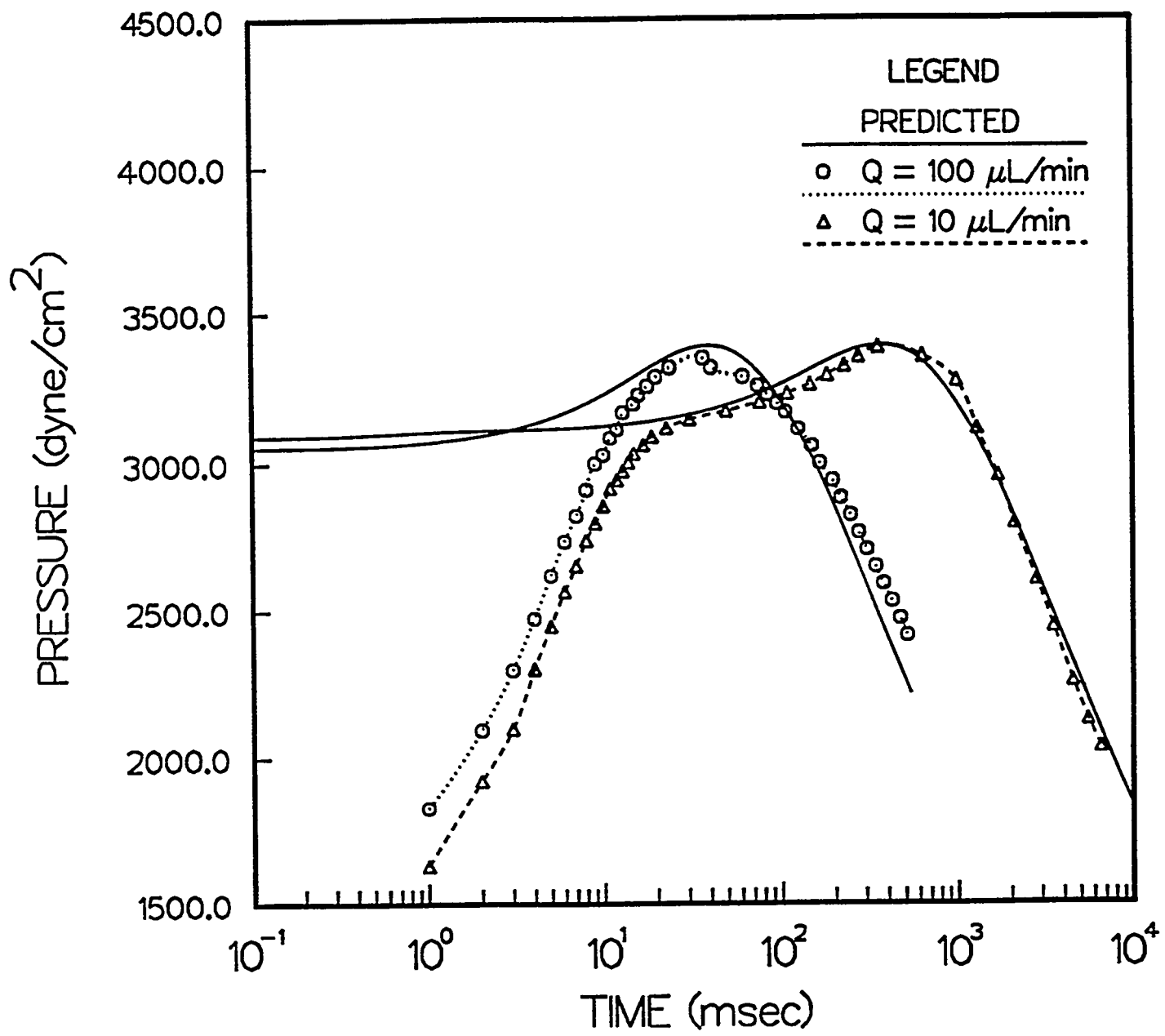


Figure 15. Zhang *et al.*

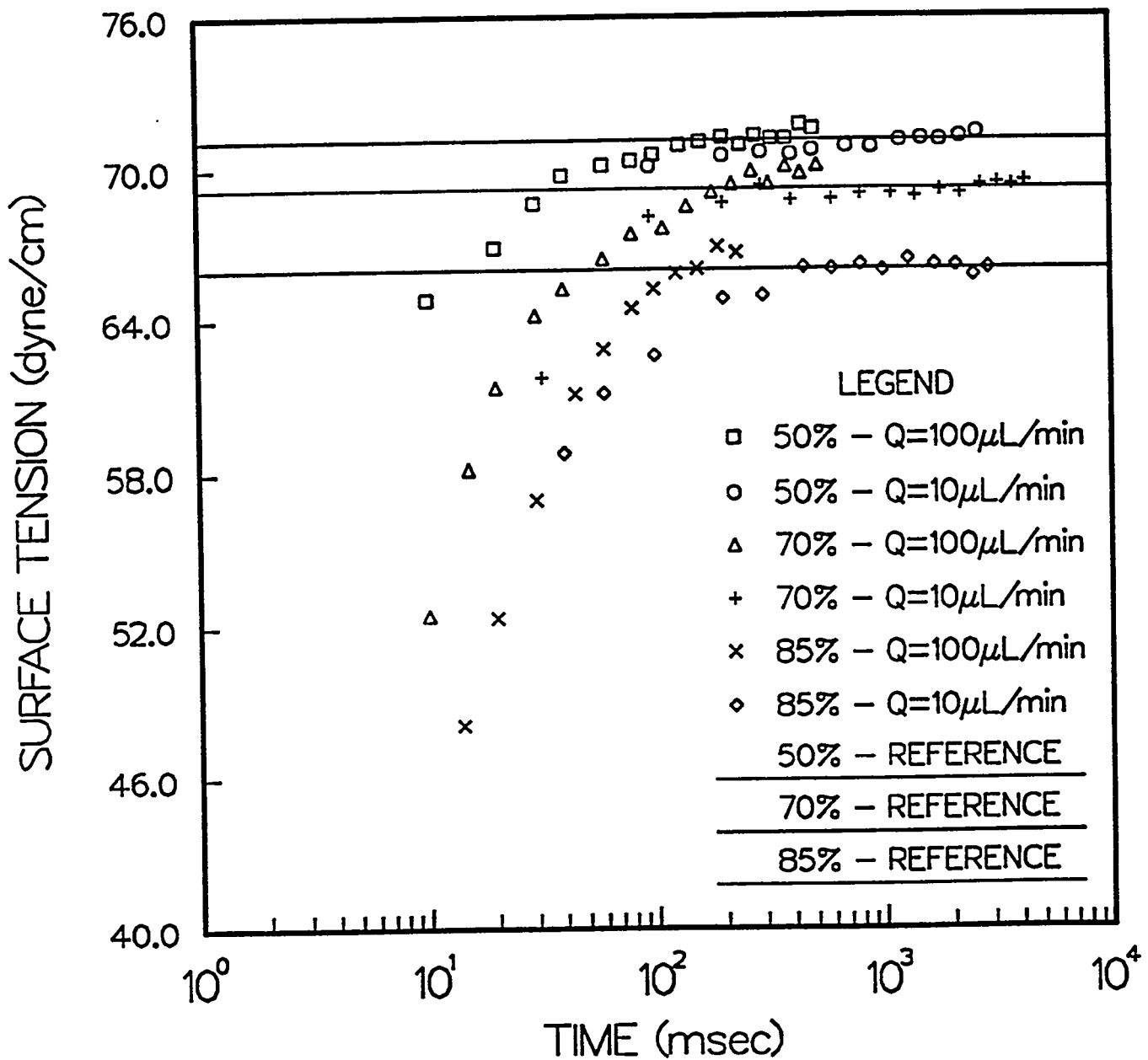


Figure 16. Zhang *et al.*